Geologic controls on paleodrainage incision and morphology during sea level lowstands on the Cascadia shelf in Oregon, USA

Authors and Affiliations: Shannon Klotsko[a,b], Matthew Skakun[b], Jillian Maloney[b], Amy Gusick[c], Loren Davis[d], Alexander Nyers[e], David Ball[f]

[a]Department of Earth and Ocean Sciences, University of North Carolina Wilmington, 601 S. College Rd., Wilmington, NC 28403, USA

[b]Department of Geological Sciences, San Diego State University, San Diego, CA, USA

[c]Natural History Museum of Los Angeles County, Department of Anthropology, 900 Exposition Blvd., Los Angeles, CA, 90007 USA

[d]Department of Anthropology, Oregon State University, 203 Waldo Hall, Corvallis, OR, 97331 USA

[e]Northwest Archaeometrics, PO Box 2427, Corvallis, Oregon, 97339, Corvallis, OR, USA

[f]U.S. Department of Interior, Bureau of Ocean Energy Management, 760 Paseo Camarillo, Suite 102, Camarillo, CA, 93010 USA

Corresponding Author: Shannon Klotsko, klotskos@uncw.edu

Permanent Address: 601 S College Rd, Wilmington, NC 28403

Highlights

- On an active margin, controls on cross-shelf drainage system morphologies can change over short distances
- Antecedent structural trends can form or impede cross-shelf drainage valleys
- Subaerial exposure of convex changes in gradient is an important control on fluvial incision

Abstract

The lowstand extensions of two fluvial systems from the Cascadia subduction margin are investigated using high-resolution seismic reflection data to determine the relative controls on paleodrainage morphology. We document distinct differences between the two systems, located ~40 km apart, attributed to underlying structure and lithology, shelf gradient, and drainage basin characteristics. A cross-shelf valley exists for only one of the drainage systems, the Umpqua River. The outer shelf part of the valley is a syncline, which formed a natural structural low for lowstand drainage, while the inner shelf part of the valley exhibits incision and is associated with a mid-shelf convex change is slope. The other drainage system, the Siuslaw River, did not develop an across-shelf valley and is only denoted in the seismic data by an erosional subaerial unconformity. Structural trends are perpendicular to cross-shelf drainage, supporting a more anastomosing stream morphology for the paleo-Siuslaw. The shelf edge for this system was not exposed for a long period of time during the last lowstand, preventing substantial outer shelf incision. Differences in fluvial elevation, discharge, and hinterland geology, also played a role in the cross-shelf morphologies of the paleo-Umpqua and

paleo-Siuslaw. These results highlight how controls on lowstand paleodrainage morphology can change over short distances on an active margin.

Keywords

Shelf (morphology and stratigraphy), active continental margin structure/tectonics, geophysics (seismic), Quaternary stratigraphy, NE Pacific, fluvial incision

1. Introduction

Fluvial response to sea-level variability during late Quaternary glacial-interglacial cycles is recorded on continental shelves worldwide (Zhang and Li, 1996; Posamentier, 2001; Burger et al., 2001; Nordfjord et al., 2006; Crockett et al., 2008; Chaumillon et al., 2010). Early sequence stratigraphic models, based primarily on passive margin settings, proposed that streams incise into the continental shelf during sea level fall and aggrade during sea level rise (Posamentier & Vail, 1988; Van Wagoner et al., 1988). Numerous refinements to those models have demonstrated that fluvial response to sea-level change is controlled by several factors including tectonics, climate, basin characteristics (e.g., size, sediment supply, discharge volume), and shelf physiography (e.g., Schumm, 1993; Wescott, 1993; Zaitlin et al., 1994; Talling, 1998; Blum et al., 2013; Wang et al., 2019). These factors not only control if fluvial incision or bypass occurs, but valley width and incision depth as well (Talling, 1998; Blum et al., 2013; Wang et al., 2019). Records of fluvial incision and infilling are important for understanding long-term sediment transport from land to sea and associated biogeochemical cycling and hydrocarbon reservoirs (Vail et al., 1977; Van Wagoner et al., 1988; Zaitlin et al., 1994). Additionally,

66 paleodrainage systems can record environmental response to climate change and be associated
67 with early archaeological resources (e.g., Minor and Toepel 1986; Punke and Davis 2006; Gusick
68 and Faught 2011; Davis et al. 2019).

69 While numerous studies of submerged paleodrainage systems have been conducted
70 along passive margins (e.g., Suter and Berryhill, 1985; Foyle and Oertel, 1997; Boss et al., 2002;
71 Simms et al., 2006; Nordfjord et al., 2006; Chaumillon and Weber, 2006; Chaumillon et al.,
72 2008; Green et al., 2013; Tesson et al., 2015; Weschenfelder et al., 2014; Aquino da Silva et al.,
73 2016; Bae et al., 2018; Liu et al., 2018), there are few detailed studies about paleodrainages
74 along active margins (Posamentier, 2001; Burger et al., 2001; 2002; Wilson et al., 2007; Maselli
75 and Trincardi, 2013; Gobo et al., 2014; Alqahtani et al., 2015). Of those studies, most have
76 examined onshore systems or focused on valley infill deposits and processes (Wilson et al.,
77 2007; Twitchell et al., 2010; Maselli and Trincardi, 2013; Gobo et al., 2014). Additionally, the
78 effects of an active margin on paleodrainage morphology can vary widely within an entire
79 region and between tectonic regimes (Posamentier, 2001; Burger et al., 2001; 2002; Twichell et
80 al., 2010; Maselli and Trincardi, 2013; Alqahtani et al., 2015). To understand better the relative
81 factors influencing paleodrainage morphology on active margins, additional case studies from
82 distinctive tectonic settings are needed. The continental shelf along a convergent margin offers
83 a valuable perspective on fluvial evolution because of the inherent complex morphology caused
84 by subduction and impacts from cycles of tectonic subsidence, associated with ruptures, and
85 long-term uplift. This setting provides a clear window into the way geological control can act on
86 valley development and filling. To investigate these impacts, we examined the continental shelf
87 offshore from two drainage systems (Umpqua and Siuslaw rivers) in central Oregon, USA,

88 located just inshore of the Cascadia subduction zone along the North Pacific coast of North
89 America (Figs. 1 and 2).
90 The Cascadia continental shelf is an ideal study location due to the influence of millions
91 of years of tectonic activity on shelf geomorphology. Most of the shelf was exposed subaerially
92 when sea level was lower during the last glacial maximum (LGM; Fig. 3); it was ~147 m below
93 modern sea level in the study area based on a regional glacial isostatically adjusted sea level
94 curve (Clark et al., 2014). Notably in central Oregon, there were large headlands and
95 embayments during the lowstand, in contrast to the relatively linear modern shoreline (Figs. 2
96 and 3). Because of subduction and other localized faulting, there is also alongshore variation in
97 geology and uplift (Kelsey et al., 1996), which can have substantial impacts on fluvial incision
98 (Wang et al., 2019). Here, we aim to demonstrate the effects of a convergent margin on
99 paleodrainage morphology with the goal of furthering our understanding of the relative
100 controls on fluvial incision on active margins during the Quaternary.
101
102 **2. Regional Setting**
103 *2.1 Tectonics*
104 The study area in central Oregon is located within the forearc of the Cascadia
105 subduction zone (Fig. 1), where the southern portion of the Juan de Fuca Plate is subducting
106 below the North American Plate at a rate of ~3-4 cm/yr (DeMets et al., 1990; Miller et al.,
107 2001). The region has experienced 12 megathrust earthquakes (magnitude 8-9) in the last 6700
108 years, each resulting in coastal coseismic subsidence up to 3 m, based on onshore stratigraphy
109 and diatom assemblages (Witter et al., 2003; Milker et al., 2016). The offshore turbidite record

110 indicates 19 margin-wide paleoseismic events over the Holocene, resulting in an average
111 recurrence interval of ~500 to 530 years, while smaller, segmented paleoseismic events
112 terminating around Heceta Bank (Fig. 2) have a recurrence of 300-380 years (Goldfinger et al.,
113 2012). This frequency may extend into the latest Pleistocene, but the turbidite record is
114 dominated by sediments of non-seismogenic origin (Goldfinger et al., 2012). Despite periods of
115 coseismic subsidence, the coast is experiencing long term uplift, as evidenced by Quaternary-
116 aged marine terraces in the Oregon Coast Range (McInelly and Kelsey, 1990; Muhs et al., 1990;
117 Kelsey and Bockheim, 1994; Kelsey et al., 1996). Uplift rates in central Oregon range
118 latitudinally from quite low (0 – 0.2 m/ky; Kelsey and Bockheim, 1994) within much of the study
119 area to significantly higher about 20 km to the south at Cape Arago (Fig. 3; 0.5-0.77 m/ky;
120 McInelly and Kelsey, 1990; Simms et al., 2016) and about 45 km to the north at Yaquina Bay
121 (Fig. 3; 0.75-0.96 m/ky; Kelsey et al., 1996; Simms et al., 2016). This part of coastal Oregon has
122 had an increase in the uplift rate since 120 ka, which has caused a transient response in the
123 regional river systems (Whipple and Tucker, 2002; VanLaningham et al., 2006).
124
125 *2.2 Shelf Geology and Structure*
126 The modern shelf, in the majority of the study area, ranges in width from 25 to 35 km from
127 the modern shoreline to the shelf break. Notably, the shelf extends to 70 km in width at Heceta
128 Bank (Fig. 2). The shelf edge occurs in ~150 m water depth (Figs. 1 and 2). The current
129 continental shelf in central Oregon formed primarily as a result of subduction zone processes
130 and was originally part of the Neogene Cascadia forearc basin, which is the subject of McNeill et
131 al. (2000). Based on this study, the base of the shelf is composed of a combination of Siletz

River volcanic rocks (large Eocene-aged basaltic flows exposed in coastal Oregon; Snavely and Baldwin, 1948) and Paleogene mélange, overlain by basin fill sediments. The forearc basin, bounded to the west by an anticlinal outer arc high and to the east by the Coast Range, was filled with sediments during sea level high stands and has been eroded, deformed, and refilled with marine and terrestrial sediment through time to form the modern continental shelf.

In this region, the shelf structure is dominated by folds and faults formed by Miocene and younger compression adjacent to the plate boundary (Fig. 4; Goldfinger et al., 2014). Axes of the major anticline and syncline systems on the shelf trend NE-SW, or slightly NW-SE (Fig. 4; Clarke et al., 1985). Miocene rocks are exposed at the seafloor where they have been uplifted, forming submarine banks (Figs. 1, 2 and 4; McNeill et al., 2000). Heceta Bank is one of these features and denotes the only location where the outer arc high has been uplifted enough to form part of the modern shelf. Heceta Bank backs up to Siletzia (a large igneous province in the coastal Pacific Northwest of North America, which was accreted to the continent in the Eocene; Wells et al., 2014), and may have contributed to its high uplift rate. Alternatively, Heceta Bank may have formed via a series of thrust faults (Seely et al., 1974). The most recent episode of deformation in this region started in the Pliocene and extended into the Pleistocene (Clarke et al., 1985). No significant tectonic deformation has occurred since, but Heceta Bank was truncated during Pleistocene sea level lowstands (Clarke et al., 1985). Siltcoos Bank, a much smaller, mid-shelf feature in the center of our study area (Fig. 2), is also composed of Miocene-Pliocene rocks (Fig. 1), and was likely uplifted by an active reverse fault (McNeill et al., 2000). Pliocene rocks and Pleistocene sediments overlay the Miocene structure, where it is not uplifted to the seafloor (Fig. 1; Clarke et al., 1985). The Pleistocene sediments have been

154 sampled and analyzed in multiple studies; they have been described as sand and silt
155 interbedded with some gravel (Snavely et al., 1977; 1981), clayey silt with a large amount of
156 coarse debris (Kulm et al., 1973), and fine silt and clay (Clarke et al., 1985).
157
158 *2.3 Characteristics of Drainage Systems*
159 The Siuslaw and Umpqua Rivers drain the central Coast Range of Oregon (Fig. 1). Table 1
160 summarizes their modern drainage basin characteristics. The Siuslaw River is of moderate size,
161 but the Umpqua River is one of the larger river systems in central Oregon. The Siuslaw River
162 primarily flows over the Tyee Formation, an Eocene layered marine sandstone/siltstone that is
163 soft and easily erodible (Walker and MacLeod, 1991; Siuslaw Basin Council, 2002; Santra et al.,
164 2013), making up most of the Coast Range (Fig. 1). This soft material is subject to large debris
165 flows in the rainy season, allowing the river to incise a low-gradient path through the steep
166 Coast Range. The Siuslaw does not have any large man-made dams that impede its drainage
167 patterns or affect sediment yield (Table 1). However, this is not the natural state of the river, as
168 extensive natural logjams were observed by early European explorers in the area (Siuslaw Basin
169 Council, 2002). Settlers in the late 1800s removed many of these log jams, causing the Siuslaw
170 to become more channelized and removing much of its ability to store water in its upper
171 reaches. This resulted in more stream incision, separating the channels from floodplains and
172 wetlands, leading to more seasonality in drainage volume (wet winters with high drainage and
173 dry summers with low drainage) and increasing the frequency of debris flows. Prior to this, the
174 drainage system would have had a more complex network of channels and wetlands, which
175 allowed water to be stored longer into the dry season. Yet, the seasonality of discharge is also

bolstered by the low elevation of the Coast Range, which does not support an extensive snowpack and leads to a short time span between precipitation events and drainage to the sea; event driven, or flashy drainage.

The Umpqua River, in contrast, drains a variety of terrains (Fig. 1), leading to less event-driven flows, but still with higher discharge volumes in the winter versus the summer (Wallick et al., 2011). The Umpqua River has a number of hydroelectric dams and reservoirs on its upper reaches (North and South Umpqua rivers), but this has little effect on downstream flow patterns and overall annual discharge because most of the basin lies below these dams. The Umpqua River has two main tributaries, the North Umpqua River and the South Umpqua River. The North Umpqua originates in the Cascades province (Fig. 1), flowing over Pliocene and Quaternary volcanic rocks that are highly permeable, providing high groundwater storage that supports consistent summer drainage (Jefferson et al., 2010). Both rivers flow through the western part of the Cascades province (Fig. 1) with Tertiary volcanic rocks that have high runoff rates (Stillwater Sciences, 2000) and through the Klamath Mountains (Fig. 1), composed of Mesozoic metamorphic rocks (Wells et al., 2001). The confluence of the two rivers, forming the Umpqua River, is near the Klamath Mountains-Coast Range boundary (Fig. 1). From there, the Umpqua primarily flows over the Tyee formation, incising into the soft sediment (Wallick et al., 2011).

The modern coast of central Oregon has a temperate (3° C – 20° C), maritime climate. Precipitation rates, which impact discharge and vegetation, as well as influence sediment erosion and transport, only vary slightly across the study area. The average annual precipitation for coastal Oregon is 212 cm, based on data collected from 1901 to 2020 (NOAA, 2020). This

198 region is located in the southern reaches of the Western Hemlock zone, a densely vegetated,
199 coniferous forest starting in coastal British Columbia (Pojar et al., 1991). The vegetation has
200 varied since, and even during, the last glacial period, but has typically included various firs,
201 pines, and hemlocks, fluctuating based on temperature and precipitation (Worona and
202 Whitlock, 1995). Overall, the dominant vegetation during the last glacial period indicated a
203 colder, more arid regional climate, with the Coast Range being ~50% drier than today during
204 the glacial-interglacial transition (25 ka to 17 ka; Worona and Whitlock, 1995).
205
206 **3. Methods**
207 In May and September 2017, ~1,075 km of Chirp subbottom and sidescan sonar data were
208 collected on R/V *Pacific Storm* to characterize the paleolandscapes offshore from the modern
209 Siuslaw and Umpqua Rivers (Fig. 2). Scripps Institution of Oceanography's Edgetech 4200
210 sidescan was used for both cruises; data were recorded in JSF format along with real-time GPS
211 for position accuracy. The data were processed using Xsonar (Danforth, 1997), which accounts
212 for slant range beam angle distortion, merges navigation with the data, and generates a
213 mosaiced image.
214 An Edgetech 512i Chirp was used for each cruise. The system used for the May 2017 cruise
215 was operated with a 30 ms swept pulse of 0.5-7.2 kHz. These data have two types of data
216 artifacts, (1) repeated diagonal lines and (2) a wavy, undulating signal, and both interfere with
217 real data at times. The September 2017 cruise used Scripps Institution of Oceanography's
218 towfish, operated with a 30 ms swept pulse of 1-15 kHz. Additional 3.5 kHz subbottom data
219 collected during cruise NA087 on E/V *Nautilus* were used to help constrain features in the

220 northern part of the study area (http://www.nautiluslive.org/science/data-management). All
221 subbottom data were recorded in SEG-Y format, along with real-time GPS data for position
222 accuracy. These data were processed using SIOSEIS (Henkart, 2006), plotted using Seismic Unix
223 (Cohen and Stockwell, 1999), and then imported into the Kingdom software package
224 (kingdom.ihs.com) for interpretation. A nominal velocity of 1500 m/s was applied to convert
225 two-way travel time (TWTT) to depth;.
226 Onshore fluvial profiles were generated based on where mapped river locations (USGS
227 National Hydrography Dataset; https://www.usgs.gov/core-science-systems/ngp/national-
228 hydrography) crossed NOAA's National Centers for Environmental Information (NCEI) Central
229 Pacific and Northwest Pacific Digital Elevation Models (DEM) with 3 arc-second resolution and a
230 mean high water (MHW) datum (NGDC, 2003a; NGDC, 2003b). Continental shelf profiles,
231 projected roughly perpendicular to depth contours from the mouth of each river to the LGM
232 shoreline, were modeled based on depths from the NCEI DEMs for the Central Oregon Coast
233 (Carignan et al., 2016) and Port Orford (Carignan et al., 2009). These both have a cell size of 1/3
234 arc seconds and a MHW vertical datum. The thalweg of the Umpqua paleovalley was mapped
235 based on chirp data. Percent-slope calculations along profiles are calculated in between
236 inflection points. The paleoshoreline contours are modeled based on relative sea level curves
237 developed by Clark et al. (2014).
238
239 **4. Results**
240 *4.1 Acoustic Properties of Submerged Paleodrainages*

241 There is a large infilled valley system offshore from the modern Umpqua River. The valley is
242 mapped in modern water depths of ~80 to 150 m (Fig. 4). The acoustic character of the system
243 (bottom reflector shape and acoustic character, fill thickness and character) varies throughout
244 its extent (Figs. 5-10). On the inner shelf, the valley bottom reflector ranges from nearly flat to
245 undulating to sharply curved (Figs. 5, 8, and 9), reflecting clear incision into the underlying
246 bedrock. In this area, the valley fill is thinnest (<10 m), but there may have been some
247 truncation by wave action during sea level transgression (Figs. 5, 7-9). In this area, The fill is
248 primarily acoustically transparent, but sometimes has internal reflectors indicative of
249 progradation or migration of incision (Figs. 5, 7, and 9), typical of an incised valley.
250 As the valley system extends to the outer shelf, it increases in depth, with fill up to ~25 m
251 in thickness (Figs. 4-6, 9, and 10). The valley also widens here, covering at least 13 km in the N-S
252 direction (Figs. 4 and 6). The valley system bifurcates around structural highs that extend to the
253 seafloor and protrude as hardground pinnacles (Figs. 4 and 10). These are described in section
254 4.2. The valley bottom reflector ranges from low to high amplitude and has an irregular, uneven
255 appearance (Figs. 4-7). The outer shelf valley fill is either acoustically transparent or has internal
256 layered reflectors (Figs. 4-6, 9). These reflectors are typically medium to high amplitude and
257 sometimes onlap the valley wall (Fig. 6). The overall paleodrainage incision depth increases
258 towards the southwestern portion of the study area (Figs. 9 and 10), near the shelf break-slope
259 transition, associated with greater valley fill thickness (Fig. 4). A smaller channel with thinner fill
260 extends from the outer shelf part of the valley to the northeast, offshore from Tahkenitch Lake
261 (Figs. 2 and 4).

262 Offshore from the modern Siuslaw River, there is not a definable incised drainage channel
263 or valley. There is, however, a distinctive medium-to-high amplitude reflector that has an
264 almost blotchy acoustic character (Fig. 11). The reflector truncates the small number of features
265 that are imaged below it; in general, little stratigraphy is imaged in the northern portion of the
266 study area. This reflector has an irregular, undulating appearance, both broadly shallowing and
267 deepening, and is hummocky at a smaller scale (Figs. 12 and 13). This is typical of an erosion
268 surface (Lobo et al., 2018), and the reflector is denoted as such (Erosion Surface; ES). The ES
269 ranges from ~6 m below the seafloor to occasionally merging with the seafloor, but it is
270 primarily within 3 m of it (Figs. 11 and 12). The ES is mapped throughout the northeast portion
271 of the study area (Fig. 4), extending from ~125 mbsl offshore, to the eastern limit of the seismic
272 data at ~55 mbsl. Beyond the shelf break offshore from the Siuslaw is a sediment wedge over 5
273 m thick (Fig. 12).
274
275 *4.2 Structure and Shelf Morphology*
276 There is complex structure throughout the study area (Fig. 4). Folded and dipping strata of
277 varying geometries are imaged in this region, including syncline-anticline structures (Figs. 6-7
278 and 9-10). The more well-defined, offshore portion of the Umpqua valley system often
279 coincides with the location of syncline fold axes (Figs. 6 and 10). Around Siltcoos Bank, the
280 steepness of dipping beds increases, and strata are folded more tightly (Figs. 6 and 10).
281 Often, structures from the underlying strata protrude above the surrounding seafloor in
282 the form of hardgrounds (Figs. 4-6 and 8-10). These were mapped where they protrude, as well
283 as where they extend upwards and come within 0.015 s TWTT of the seafloor (Fig. 4). Where

284 imaged, these protruding hardgrounds have higher backscatter compared to the surrounding
285 seafloor (Fig. 4) and higher acoustic amplitude (Figs. 5, 8, and 10). In the Chirp data, the
286 exposed hardgrounds range from mound-like (Figs. 5 and 8) to narrower and more pinnacled
287 (Figs. 5-6 and 9-10). When they protrude above the surrounding seafloor, the hardgrounds
288 sometimes trend in a linear fashion (Fig. 4), particularly in the southern region, but have either
289 a modular or widespread coverage in other areas. Hardgrounds are most common in the
290 middle and outer shelf (Fig. 4), between the Siuslaw and Umpqua rivers. On the outer shelf,
291 hardgrounds are mostly exposed, but some are covered by a thin veneer of sediment (Figs. 4
292 and 8-10). Hardgrounds that do not extend above the surrounding seafloor also tend to have
293 higher acoustic amplitude in Chirp data (Figs. 5, 8, and 10). In general, hardgrounds occur at
294 anticlinal axes (Fig. 4; Goldfinger et al., 2014) or are associated with folded and faulted
295 reflectors (Figs. 6 and 10).
296 Profiles of the shelf bathymetry extending from the modern shoreline at the mouth of each
297 river to 200 mbsl show notable differences between the Siuslaw and Umpqua regions (Fig.3).
298 Both have breaks in slope at the base of the coastal prism, but the Umpqua's is more
299 pronounced, as the prism extends to ~80 mbsl with over a 3% slope. The Siuslaw's coastal prism
300 extends to ~25 mbsl with a slope of 2.44%. The rest of the Siuslaw shelf profile is more gradual
301 and exhibits a gentle break in slope of 0.56-0.25% at 100 mbsl. There is a slope change on the
302 outer shelf at ~147 mbsl, nearly coincident with the 20 ka (Fig. 3). The shelf profile for the
303 Umpqua gradually transitions in slope at the base of the coastal prism from 0.57% to 0.19%
304 (Fig. 3). There is an outer shelf change in slope at ~125 mbsl from 0.19% to 0.87%. The
305 paleovalley thalweg (Fig. 3), based on the chirp data, is plotted along the same distance profile

306 as the Umpqua shelf for comparison. There are multiple slope changes, but two of those are
307 convex, one from 0.05% to 0.37% at ~95 mbsl and one from 0.03% to 0.55% at ~105 mbsl.
308
309 **5. Discussion**
310 *5.1 Interpretation of Paleodrainage Morphology*
311 The valley system offshore from the Umpqua River likely represents drainage from the
312 paleo-Umpqua River. This drainage valley is multifaceted in both character and location. The
313 inner shelf portion exhibits cut and fill features (Figs. 5 and 7) typical of an incised valley (e.g.,
314 Dalrymple, 2006; Blum et al., 2013; Green et al., 2013) and is interpreted as such, attributed to
315 lowstand fluvial incision and migration. The outer-shelf, wider and deeper portion of the valley,
316 with thick infill, is more complex. The origin of this part of the valley was unlikely due to
317 continental drainage, but rather, underlying structure, discussed in Section 5.2. This part of the
318 valley; however, does have a scoured bottom reflector (Figs. 5 and 6), which is attributed to
319 drainage from the paleo-Umpqua overprinting this surface. The thick and layered valley fill with
320 undulating reflectors are inferred as paleo-Umpqua scour and fill. The smaller portions of the
321 valley extending from the outer shelf towards the northeast are interpreted as tributaries
322 related to drainage from Tahkenitch Lake (Figs. 4 and 13).
323 There are no definitive age constraints on valley formation or fill deposition. The outer
324 shelf part of the valley could be quite old, with one of the shallower reflectors representing the
325 LGM subaerial unconformity and overall deposition related to multiple lowstand-highstand
326 cycles. Alternatively, the base of the valley could represent the LGM subaerial unconformity
327 with valley fill deposited since. Estimations of sediment accumulation rates for the modern

328 Umpqua River range from 1.4 to 2.3 mm/yr (Wheatcroft and Sommerfield, 2005). Using the
329 approximate maximum thickness of valley fill (25 m), accumulation would have taken 10.87 ky
330 and 17.86 ky based on these rates, respectively. Most of the valley fill is thinner than this,
331 requiring less time for deposition. There is no defined submarine canyon on the upper
332 continental slope here, possibly due to a large quantity of sediment blanketing the slope,
333 delivered via the paleo-Umpqua. Our subbottom data does not extend over the slope, however,
334 so this inference is based on the seaward thickening wedge of sediments imaged on the outer
335 shelf (Figs. 9 and 13). The inner shelf incised valley could be LGM in age or could have formed
336 during a previous lowstand and was reoccupied during the LGM. It is also possible that no
337 incision occurred during the last lowstand, but without sedimentary age constraints, we prefer
338 the LGM incision or reoccupation interpretation.
339 The ES is mapped offshore from the modern Siuslaw River (Fig. 4), in waters from ~55 to
340 125 m depth. This surface likely represents drainage from the paleo-Siuslaw River. Alternatively,
341 it could be the regional wave-transgressive surface, but the variability in acoustic character
342 (amplitude, undulating and hummocky surface; Fig. 11) and location relative to the modern
343 Siuslaw River, suggest that this surface is a subaerial unconformity (Zecchin and Catuneau,
344 2013), originally formed via continental drainage during the LGM lowstand. Surfaces described
345 similarly have been classified as erosional sequence boundaries of fluvial origin (Miall, 2014;
346 Lobo et al., 2018). The ES extends over ~19 km^2 (~20 km in the north-south direction), a slightly
347 larger area than the Umpqua valley (~17 km^2), yet there is no evidence of valley incision (Fig. 4).
348 The presence and irregular pattern of the ES indicates that the paleo-Siuslaw probably had a
349 shallow, potentially anastomosing stream morphology, which would have generated a network

of channels over a larger area (Miall, 2014). This would have led to overall sediment bypass of the shelf during the lowstand (Posamentier, 2001), which is supported by the scarcity of surficial sediment across the shelf in the Siuslaw region (Figs. 11 and 12), but a sediment wedge imaged past the shelf edge (Fig. 12). Such outer shelf and slope wedges are common, often associated with forced regression or lowstand fluvial deposition, or reworking of outer shelf deposits during transgression (Labaune et al., 2010; Green et al., 2013; McClung et al., 2016; Lobo et al., 2018). The shelf physiography here also forms an embayment for sediment to accumulate in on the slope (Fig. 2).

5.2 Structural Controls on Paleodrainage Morphology and Valley Formation

Long-term tectonic forces in the study region have formed a continental margin with complex geology and physiography, which appears to have influenced fluvial morphology across the shelf. The underlying structure plays a large part in location of the paleo-Umpqua drainage valley (Fig. 4). The outer shelf part of the valley, with the thickest fill, follows syncline location, which is expected, as erosion of syncline layers creates a natural low for a channel to follow and continue to incise (Figs. 4-7, 10, and 15). Synclines on the central Oregon shelf are also typically composed of Quaternary siltstones and sandstones that are poorly indurated, making them more easily erodible relative to the surrounding material (Fig. 1; Clarke et al., 1985; Peterson et al., 1986). The synclines also form a wide valley, extending over 14 km across. The deepest parts of the valley, around syncline axes, are typically more than 4 km across (Figs. 6 and 10). The hardgrounds that extend towards/protrude above the seafloor, often at anticline axes (Figs. 4 and 10; Goldfinger et al., 2014), are Miocene-Pliocene rocks that have been

372 uplifted above active folds and fault zones (Figs. 1 and 4; Clarke et al., 1985; McNeill et al.,
373 2000). These have been mapped as two different geologic units based on deep-penetration
374 seismic reflection data and samples (Fig. 1; Clarke et al., 1985; Peterson et al., 1986). The rocks
375 uplifted just south of the Umpqua River and those at Siltcoos Bank are interpreted as late
376 Eocene to middle Miocene marine sedimentary rocks, with some volcanic rocks interbedded
377 (Fig. 1; Clarke et al., 1985; Peterson et al., 1986); potentially the Astoria Formation, a hard,
378 fossiliferous-rich marine rock (Snavely, 1987; Goldfinger et al., 2014). The broader region
379 around Siltcoos Bank is mapped as late Miocene to late Pliocene mudstone and siltstone with
380 some sandstone (Fig. 1; Clarke et al., 1985; Peterson et al., 1986). These features are more
381 resistant to erosion than the younger, overlying Quaternary sediments (Clarke et al., 1985),
382 which can affect channel incision (Chaumillon et al., 2008). In the shallower areas, the Umpqua
383 paleodrainage valley exhibits clear deepening and downcutting of channels that terminate
384 against the hardgrounds (Figs. 5 and 13). Additionally, valley fill thickness increases towards the
385 outer shelf as the orientation of bedrock layers changes and they dip towards the shelf edge
386 (Fig. 9). These observations highlight the role that lithology and structure play in drainage
387 patterns and incision.

388 Similar geologic controls on drainage valley morphology have also been observed along
389 other margins (Chaumillon et al., 2008; Tesson et al., 2015; Lobo et al., 2018). The submerged
390 paleo-Charente River on the French Atlantic coast has a seaward distributary pattern with
391 thalweg jumps attributed to tectonics (Weber et al., 2004). Folded and faulted Mesozoic
392 bedrock underlies the drainage system and incised channel thalwegs often coincide with
393 synclinal bedrock structures. A synthesis of incised valleys throughout the Bay of Biscay

394 highlights tectonic control on valley orientation, as they are primarily aligned with faults and
395 fault scarps (Chaumillon et al., 2008). Many of these systems also preferentially incised soft
396 sediment while abutting harder strata. On the French Mediterranean coast, the incised valley of
397 the paleo-Aude and -Orb rivers runs shore parallel, in the direction of seaward dipping layers,
398 and lacks substantial incision depth due to a shallow and relatively flat plateau (Tesson et al.,
399 2015). The paleo-Chao Phraya-Johore River valley on the Sunda Shelf parallels basement
400 structure associated with subsidence and has tributaries oriented along extensional faults
401 (Alqahtani et al., 2015). In the Gulf of Cádiz, fluvial incision patterns and the morphology of the
402 LGM subaerial unconformity reflect a distinct change between the inner and outer shelf,
403 attributed to lithologic differences in the two regions (Lobo et al., 2018).
404 Based on our observations and comparison with these other drainage systems, we infer
405 that the primary control on the morphology of the paleo-Umpqua drainage valley is the
406 antecedent topography and lithologic differences generated by the tectonic history of the
407 Cascadia margin. The structural patterns (folding and faulting) formed a natural valley across
408 the shelf for the paleo-Umpqua to follow and lithology played a role in valley depth, as incision
409 and valley deepening is greater in softer Pleistocene sediments (Clarke et al., 1985) compared
410 to older, harder material.
411 The trend of folding offshore from the Siuslaw River is different than offshore of the
412 Umpqua River. Folding is oriented in a more NNW-SSE direction (Fig. 4), forming structural lows
413 that are nearly perpendicular to a Siuslaw cross-shelf drainage pathway. This trend likely
414 promoted an anastomosing system, with multiple channels distributed along fold axes,
415 generating the wide-ranging ES with extensive, yet variable scour.

416

417 *5.3 Physiographic Controls on Paleodrainage Morphology*

418 Previously developed sequence stratigraphic models suggest that shelf physiography
419 (shelf gradient and shelf break depth) is a major control on incised valley development
420 (Summerfield, 1985; Posamentier et al., 1992; Posamentier and Allen, 1993; Talling, 1998; Blum
421 and Törnqvist, 2000; Posamentier, 2001). In these models, the difference in gradient between
422 the fluvial profile landward of the highstand shoreline and that of the newly exposed shelf is a
423 dominant influence on fluvial incision versus aggradation, as well as channel morphology. If the
424 slope is the same between the two regions, sediment bypass is expected (Summerfield, 1985;
425 Posamentier et al., 1992; Holbrook and Bhattacharya, 2012). If the slope onshore is greater
426 than the shelf, aggradation is predicted, and if the slope onshore is less than the shelf, incision
427 is predicted (Van Wagoner et al.; 1988; Posamentier et al., 1992; Holbrook and Bhattacharya,
428 2012). Rivers may also adjust to these changes in slope by altering sinuosity, with lower
429 sinuosity when the onshore slope is greater than the shelf, and vice versa (Schumm, 1993). The
430 magnitude of the slope change will determine the level of sinuosity and/or incision. Other
431 models highlight the importance of convexity in the continental shelf profile (Talling, 1998;
432 Blum and Törnqvist, 2000). In these models, incision is only expected in cases where sea level
433 falls below a convex change in slope, typically the shelf break or the coastal prism (highstand
434 shoreline; Posamentier et al., 1992; Talling, 1998). If sea level falls below the shelf break, then
435 an incised valley should form across the entire shelf, but if sea level does not fall below the
436 shelf break, an incised valley will only develop in the vicinity of the coastal prism (Talling, 1998;
437 Posamentier, 2001; Törnqvist et al., 2006). Although the rivers studied here are located within

40 km of one another and have the same general trend in slope from onshore to offshore, the shelf profiles offshore from each modern system have localized slope variability (Fig. 3).

The Umpqua shelf profile exhibits two convex changes in gradient, one at the base of the coastal prism and the other at ~120 mbsl (Fig. 3). The deeper slope change correlates approximately with the 14 ka paleoshoreline (Fig. 3). It also represents the start of the continental shelf-slope transition, which occurs shallower and more gradually here compared to other parts of the shelf (Fig. 3). Because sea level was ~147 m below present in this region during the LGM (Clark et al., 2014), this convex change in slope would have been subaerially exposed may have contributed to additional scouring of the preexisting structural valley. The paleo-Umpqua valley thalweg profile has two convex changes in gradient on the mid-shelf, near the inner shelf incised valley. When sea level dropped below these points (105 mbsl is the deeper of the two), incision was probably initiated, influenced by overall structural patterns and lithology on the inner shelf.

The Siuslaw shelf profile represents a ramp margin with little variability in slope between the convex breaks at the coastal prism and shelf edge (Fig. 14). The shelf edge in this profile is at ~150 m water depth, but varies in the Siuslaw area between 140 and 150 m water depth. This is quite close to the calculated LGM sea level of about -147 m (Clark et al., 2014), indicating potential shelf edge exposure, which suggests incision may have occurred. The absence of valley development is typical for sea level falls that do not drop below the shelf edge or expose an outer shelf convex change in slope, which may have been the case for the paleo-Siuslaw. Plink-Björklund and Steel (2004) documented the presence/absence of incised valleys on the Eocene coastal plain and shelf of Spitsbergen due to differing magnitudes of sea level

falls. Both Simms et al. (2006) and Chaumillon and Weber (2006) describe incised valleys, in the Gulf of Mexico and the French Atlantic coast, respectively, that do not extend across the entire shelf due to a lack of outer shelf convexity. The duration of shelf exposure, however; may have been a factor in controlling incision because fluvial systems need enough time to adjust to changing slope for incision to occur (Woolfe et al., 1998; Blum et al., 2013). Because the shelf edge depth is so close to the LGM sea level, any exposure would have been for a relatively short time period and may have prevented the paleo-Siuslaw from developing substantial incision and knickpoint retreat prior to being inundated during the transgression. Abbott and Carter (1994) and Naish and Kamp (1997) have presented evidence of this in New Zealand. There, over 40 Plio-Pleistocene marine cyclothems are documented, but only two of the sequence boundaries record fluvial incision, when there was sufficient time for fluvial systems to adjust to the new equilibrium profile. In general, most rivers did not reach their equilibrium profile during the most recent lowstand, even those that formed incised valleys (Strong and Paola, 2008; Wang et al., 2019). The lack of a distinct cross-shelf incised valley for the paleo-Siuslaw can be principally attributed to the shelf's localized ramp morphology and insufficient exposure of the shelf break during the last lowstand. Instead, this likely resulted in overall sediment bypass for most of the glacial period (e.g., Talling, 1998 model), with slight scouring of the existing surface, forming the ES (Schumm, 1993).

Based on shelf-fluvial profile comparisons, we infer that shelf morphology, and relation to sea level, exerts strong control on fluvial incision during lowstands on the Cascadia margin. When a convex slope break is exposed subaerially for a sufficient amount of time, incision can occur, but other factors may have a stronger influence on incision, as is the case for the

Umpqua outer shelf where the preexisting syncline is the dominant control on drainage system morphology. The paleo-Umpqua only incised the middle to inner shelf, where convexity in the paleovalley thalweg was exposed and the paleo-Siuslaw did not form a cross-shelf incised valley. Both, the Siuslaw and Umpqua shelf profiles are characterized by a convex slope break at the coastal prism (Fig. 3), which should have resulted in fluvial incision across the inner shelf (Talling, 1998). However, additional subbottom data is needed in this region (Fig. 2) to determine the presence or absence of incised valleys near the mouths of the Siuslaw and Umpqua rivers. Nevertheless, this would only control incision through the coastal plain and not across the full width of the shelf exposed during sea level lowstands. It is also possible that continuing tectonic activity has altered the shelf profiles since the lowstand. However, the long-term regional uplift rates are low and would have only caused a few meters of change, unlikely to have affected shelf profiles substantially (McInelly and Kelsey, 1990; Kelsey and Bockheim, 1994; Kelsey et al., 1996; Simms et al., 2016).

Lastly, it is possible that the different morphologies observed in seismic reflection data could be explained by differential preservation of each paleodrainage system, rather than by factors controlling their formation. On the Siuslaw outer shelf beyond the ES, there is almost no evidence of lowstand or falling stage surfaces, nor sediment fill or high stand sedimentation (Fig. 12). This is between the 14 ka and 20 ka paleoshorelines, when there was a slower rate of sea-level rise (Fig. 3). The ES is mapped on the portion of the shelf that was inundated during a period of rapid rise in sea level from 14 to 8 ka (Fig. 4; Clark et al., 2014). The paleo-Umpqua drainage valley is mapped between the 8 ka and 20 ka paleoshorelines. Periods of rapid sea-level rise would be more likely to preserve evidence of fluvial systems, as deposits would

quickly be submerged beyond the reach of wave base erosion. The absence of stratigraphy below the seafloor on the part of the Siuslaw shelf that was inundated during a slower rise in sea level, indicates that an incised valley may have formed, but was then obliterated during transgression. This has been observed on the KwaZulu-Natal continental shelf where rapid sea-level rise is suggested as the mechanism for partially filled incised valleys and preservation of paleoshoreline deposits, while smoothed surfaces are attributed to extensive wave ravinement during periods of slower sea-level rise (Pretorius et al., 2019; Salzmann et al., 2013).

This process is also dependent on the slope of the shelf, with respect to each drainage system, which would have influenced how long wave base erosion impacted the seafloor. In theory, a lower gradient would expose each area of the shelf to wave action for a shorter period of time compared to a steeper gradient, promoting preservation (Cattaneo and Steel, 2003). This is documented on the southeastern African shelf where paleoshoreline features are better preserved in lower gradient areas (Green et al., 2018). Between the 20 ka and 14 ka paleoshorelines, the Siuslaw shelf has a gentler slope than the Umpqua shelf profile (Fig. 3), suggesting that any Siuslaw paleodrainage features would be better preserved than Umpqua features. However, the Umpqua outer shelf valley may be so well preserved because of the valley scale. This is common along glaciated margins where large-scale valleys and geomorphic lows formed via glacial meltwater drainage were not obliterated during transgression (Hill et al., 2007; Thieler et al., 2007; Hill and Driscoll, 2008; Klotsko and Driscoll, 2018). Nevertheless, we infer that the paleo-Siuslaw did not form any substantial drainage features on the outer shelf. There may have been some minor scouring, but any evidence of this was removed during transgression. The Siuslaw shelf profile is steeper than the Umpqua shelf profile for much of the

14 ka to 8 ka paleoshoreline range (Fig. 3), suggesting poorer preservation of paleo-Siuslaw features. Some infill above the ES may have been removed and reworked during transgression, as sediment cover is quite thin here (Fig. 11). The ES, however, does not appear to have been altered by wave action where buried. The preservation of the ES on the part of the shelf inundated during rapid sea-level rise without evidence of an incised valley, supports our conclusion that the paleo-Siuslaw had a more anastomosing channel morphology across the shelf during the lowstand.

5.4 Influence of Drainage Basin Characteristics on Paleodrainage Incision and Morphology

In addition to shelf geology, shelf physiography, and sea level, there are other factors that could have contributed to the drainage morphologies of the paleo-Siuslaw and -Umpqua rivers during the lowstand. In typical sequence stratigraphic models these are related to the characteristics of each drainage basin and include, climate, tectonic regime, discharge volume, and erodibility of source sediment (Schumm, 1993; Talling, 1998; Blum and Törnqvist, 2000; Posamentier, 2001; Blum et al., 2013). Most of these factors influence stream power; higher stream power typically leads to a greater depth of incision (Schumm et al., 1984; Paola et al., 1992; Blum et al., 2013), while lower stream power could play a role in the absence of incision. These factors also affect how long it takes for fluvial systems to reach their equilibrium profile, which is related to incision (Paola et al., 1992). Because the two drainage systems are within 40 km of each other, it is unlikely that climate history contributed to the differences in their cross-shelf morphologies. Here we examine these other factors in the context of the Umpqua and Siuslaw rivers.

548 The tectonic regime of a drainage system influences many factors related to stream power.
549 Along active margins, such as Cascadia, there is typically a narrower, steeper shelf and a coastal
550 mountain range. Coastal mountains have a higher gradient than a lowland coastal plain,
551 commonly found on passive margins, which adds to stream power. The Umpqua River descends
552 over 1800 m in elevation throughout its path to the ocean, whereas the Siuslaw is below 200 m
553 of elevation for its entire length (Siuslaw Basin Council, 2002). This is because the Siuslaw
554 effectively erodes through the uplifting Coast Range (Fig. 1), resulting in an overall low gradient
555 river with less stream power, more analogous to a passive margin river.
556 Coastal mountains support orographic precipitation (Ruddiman, 2013), and also lead to
557 rivers with smaller catchment basins than passive margins (Blum et al., 2013). However, these
558 higher elevation rivers typically have a larger discharge for their basin area (Milliman and
559 Syvitski, 1992). This effect of higher elevation is not reflected in the discharge to drainage basin
560 area ratios for the Umpqua and Siuslaw rivers (Table 1). The lower elevation Siuslaw River has a
561 smaller drainage basin than the Umpqua River (~6x), but Umpqua River discharge is only about
562 four times higher than the Siuslaw discharge (Table 1). Nevertheless, the smaller basin area and
563 discharge for the Siuslaw results in less stream power than the Umpqua. The smaller, high
564 gradient drainage basins, like the Umpqua basin, also support event driven discharge, which
565 can have more stream power than fluvial systems with more consistent discharge (Lamb et al.,
566 2015). This is further bolstered by sediment availability in mountainous areas; there is more
567 terrain to be eroded and added to the river sediment load, like the soft sediment of the Tyee
568 formation in the Oregon Coast Range (Fig. 1; Wallick et al., 2011; O'Connor et al., 2014). Even
569 though both rivers flow over the Tyee formation in the Coast Range, the Umpqua River has a

570 sediment yield more than three times that of the Siuslaw River (Table 1), which highlights the
571 impact of the more mountainous Umpqua drainage basin. All of these factors indicate a lower
572 stream power for the Siuslaw compared to the Umpqua, which may have contributed to the
573 observed lack of shelf incision by the paleo-Siuslaw.
574 Experimental and theoretical studies of bedrock erosion indicate that the grain size of
575 river sediment load can influence fluvial incision rate, with coarser gravels having the strongest
576 effect (Sklar and Dietrich, 2001; Scheingross et al., 2014; Lamb et al., 2015). The soft
577 sedimentary rocks of the Coast Range (Fig. 1) are quickly broken down into suspended load for
578 both of the rivers (O'Connor et al., 2014). A portion of the upper Umpqua also flows over the
579 more resistant rocks of the Klamath province (Fig. 1; Wells et al., 2001). Although not as large of
580 a component of the overall sediment load, Klamath rocks are more commonly transported as
581 gravels (O'Connor et al., 2014). This could also have played a factor in the degree of incision for
582 the paleo-Umpqua inner shelf valley and lack of incision for the paleo-Siuslaw.
583 An analysis of 151 late-Quaternary incised valley fills by Wang et al. (2019) found that
584 drainage basin characteristics played a significant role in incised-valley-fill dimensions. For
585 instance, a larger drainage basin area characteristically leads to a deeper and wider incised
586 valley (Mattheus et al., 2007; Mattheus and Rodriguez, 2011; Phillips, 2011; Wang et al., 2019).
587 The incised, inner shelf part of the Umpqua paleodrainage valley is ~10-15 km across. When
588 compared to seven other incised valley fills with similar drainage basin areas (10,000 and
589 15,000 km^2), most are narrower than the paleo-Umpqua (Wang et al., 2019). The one system
590 that is similar is from the Kanto Plain in Japan, which has a slightly larger drainage basin area at
591 12,900 km^2 and a valley width of ~10.4 km (Isihara et al., 2012; Isihara and Sugai, 2017; Wang et

592 al., 2019). A combination of structural trends and additional water sources are the likely
593 reasons for the larger paleo-Umpqua incised-valley-fill width. Incision imaged south of the
594 modern Umpqua river mouth was probably from Tenmile Lake (Figs. 2 and 4) outflow (adding
595 ~250 km^2 to drainage basin size; PNHM and USGS, 2020) or southward flow of the paleo-
596 Umpqua before turning offshore. Incision north of the river mouth was probably from a
597 combination of Tahkenitch Lake (Figs. 4 and 13) outflow (adding ~130 km^2 to drainage basin
598 size; PNHM and USGS, 2020) and the paleo-Umpqua, reflecting a migration of the inlet through
599 time. The mouth of the modern Umpqua River is bounded to the north by North Spit (Fig. 2), a
600 sandy extension of the natural coastal dune fields in the area and is not a rigid topographical
601 boundary. Only three of the incised valleys with similar drainage basin sizes to the Umpqua
602 examined in Wang et al. (2019) have available widths, and two of those are thicker than the
603 paleo-Umqua valley fill (<11 m; Fig. 4). These are the Apodi-Mossoro incised valley in Brazil with
604 a thickness of ~41.5 m (Vital et al., 2010; Wang et al., 2019) and the Kanto Plain in Japan with a
605 thickness of ~63 m (Isihara et al., 2012; Isihara and Sugai, 2017; Wang et al., 2019). Overall,
606 compared with the database examined by Wang et al. (2019), the paleo-Umpqua inner shelf
607 incised valley is wider and has thinner fill than most other observed valleys with a similar
608 drainage basin area. This supports the finding of Wang et al. (2019) that incised-valley-fills on
609 active margins were less likely to scale with drainage basin area than those on passive margins,
610 likely because active margins have more variability in factors affecting stream power, such as
611 gradient, drainage basin topography, and climate (Lague, 2014).
612
613 *5.5 Implications for Paleolandscape Reconstructions*

Identification of submerged terrestrial landforms along the Pacific continental shelf is important for archaeological studies of human migration into the Americas (Davis et al., 2009; Gusick and Faught, 2011; Laws et al., 2020), as evidence indicates a coastal migration pathway as early as 18-15 ka, during times of lower sea level (e.g., Davis et al., 2019; Dillehay et al., 2008; Erlandson, 2002; Erlandson et al., 2007; Fagundes et al., 2008; Gusick and Erlandson, 2019; Fedje et al., 2004; Mandryck et al., 2001). The continental shelf is a vast area to search for submerged archaeological resources, so predictive models are often employed to refine the search area (Monteleone et al., 2013; Reeder-Myers et al., 2015). Since coastal subaerial archaeological sites are often found along riverine terraces (Davis et al., 2004), submerged paleodrainages are key areas of interest for investigating early coastal migration. As such, their accurate identification and mapping are vital for improving predictive models and in identifying target search areas. Furthermore, information on the likelihood of material preservation can expressively direct archaeological search and sampling efforts. An understanding of fluvial response to sea level fluctuations and the geologic controls on site preservation are invaluable for these studies. The data and interpretations presented here can inform the developing methods for underwater archaeological research and help narrow the vast search area of the North American Pacific continental shelf, by locating preserved terrestrial landforms, especially paleodrainages.

6. Conclusions

This study improved our understanding of the dominant controls on paleodrainage morphology during lowstands and how these factors can vary greatly over short distances along convergent margins. These factors are:

(1) Underlying structure and lithology. Structural lows bounded by uplifted, harder rocks formed a natural cross-shelf valley for the paleo-Umpqua. The fold trend near the Siuslaw does not form cross-shelf structural lows.

(2) Shelf gradient. An outer shelf convex change in slope was not subaerially exposed for a sufficient amount of time for the paleo-Siuslaw to form a cross-shelf incised valley during the last lowstand. The Umpqua valley thalweg has a convex slope change on the mid shelf that may have initiated incision on the inner shelf.

(3) Drainage basin characteristics. Low stream power due to the small drainage basin, discharge, and maximum river elevation of the Siuslaw River probably played a role in the paleo-Siuslaw not forming an incised valley. The stream power of the paleo-Umpqua, bolstered by its high elevation, regional climate, and event driven precipitation supported by the orographic effect, may have led to additional deepening and widening of the preexisting structural low and inner shelf incision.

Our results highlight that adjacent rivers along the same margin can have differences in these three factors that influence their evolution. This lateral heterogeneity may be more pronounced on active margins where tectonic activity creates a variety of structures and physiography. Therefore, grouping river systems by margin type to explain their response to sea level change oversimplifies the expected paleodrainage morphology.

7. Data Availability

Per Cooperative Agreement, Final Data sets will be submitted with the draft Final Report and archived at the BOEM Pacific Region Office. NA087 data is available at http://www.nautiluslive.org/science/data-management and will also be archived at NOAA's National Centers for Environmental Information.

Acknowledgements

This work was supported by a BOEM Cooperative Agreement Award (No. M15AC00012), and a NOAA Ocean Exploration and Research Grant (No. NA16OAR0110197). The authors would like to thank the crew of R/V *Pacific Storm*, crew of the E/V *Nautilus*, N. Driscoll, H. Tahiry, and C. Nicholson for their contributions to the data collection. We also thank A.N. Green and two anonymous reviewers for their thoughtful reviewers, which helped improve the scope and clarity of this paper.

References

Abbott, S. T., and Carter, R. M., 1994, The sequence architecture of mid-Pleistocene (c. 1.1–0.4 Ma) cyclothems from New Zealand: Facies development during a period of orbital control on sea level cyclicity, in de Boer, P. L., and Smith, D. G., eds., Orbital forcing and cyclic sequences: Inter- national Association of Sedimentologists Special Publication 19, 367–394.

676 Alqahtani, F.A., Johnson, H.D., Jackson, C.A.L., Som, M.R.B., 2015. Nature, origin and evolution
677 of a Late Pleistocene incised valley-fill, Sunda Shelf, Southeast Asia. Sedimentology 62,
678 1198-1232.
679 Aquino da Silva, A.G., Stattegger, K., Schwarzer, K., Vital, H., 2016. Seismic stratigraphy as
680 indicator of late Pleistocene and Holocene sea level changes on the NE Brazilian
681 continental shelf. Journal of South American Earth Sciences 70, 188-197.
682 Bae, S.H., Kong, G.S., Lee, G.S., Yoo, D.G., Kim, D.C., 2018. Incised channel morphology and
683 depositional fill of the paleo-Seomjin River in the continental shelf of the South Sea,
684 Korea. Quaternary International 468, 49-61.
685 Blum, M.D., Törnqvist, T.E., 2000. Fluvial responses to climate and sea-level change: a review
686 and look forward. Sedimentology 47, 2-48.
687 Blum, M., Martin, J., Milliken, K., & Garvin, M., 2013. Paleovalley systems: Insights from
688 Quaternary analogs and experiments. Earth-Science Reviews 116, 128-169.
689 Boss, S.K., Hoffman, C.W., Cooper, B., 2002. Influence of fluvial processes on the Quaternary
690 geologic framework of the continental shelf, North Carolina, USA. Marine Geology 183,
691 45-65.
692 Burger, R. L., Fulthorpe, C. S., & Austin Jr, J. A., 2001. Late Pleistocene channel incisions in the
693 southern Eel River Basin, northern California: implications for tectonic vs. eustatic
694 influences on shelf sedimentation patterns. Marine Geology 177, 317-330.
695 Burger, R. L., Fulthorpe, C. S., Austin Jr, J. A., & Gulick, S. P., 2002. Lower Pleistocene to present
696 structural deformation and sequence stratigraphy of the continental shelf, offshore Eel
697 River Basin, northern California. Marine Geology 185, 249-281.

Carignan, K.S., Taylor, L.A., Eakins, B.W., Warnken, R.R., Sazonova, T., and Schoolcraft, D.C., 2009. Digital elevation model of Port Orford, Oregon: Procedures, data sources and analysis. Boulder, Colo., National Geophysical Data Center, Marine Geology and Geophysics Division, NOAA Technical Memorandum NESDIS NGDC-21, 38 p. https://www.ngdc.noaa.gov/mgg/dat/dems/regional_tr/port_orford_13_mhw_2008.pdf

Carignan, K.S., McLean, S.J., Eakins, B.W., Love, M.R., and Sutherland, M., 2016. Digital elevation model of the central Oregon coast V2: procedures, data sources and analysis. Boulder, Colorado, National Centers for Environmental Information, NOAA Technical Report, 9 p. https://www.ngdc.noaa.gov/mgg/dat/dems/regional_tr/central_oregon_13_navd88_2015.pdf

Cattaneo, A., & Steel, R. J., 2003. Transgressive deposits: a review of their variability. Earth-Science Reviews, 62(3-4), 187-228, doi: 10.1016/S0012-8252(02)00134-4

Chaumillon, E. and Weber, N., 2006. Spatial variability of modern incised valleys on the French Atlantic coast: comparison between the Charente (Pertuis d'Antioche) and the Lay- Sèvre (Pertuis Breton) incised-valleys. In: Incised Valleys in Time and Space (Eds R.W. Dalrymple, D.A. Leckie and R.W. Tillman). SEPM Special Publication 85, 57–85.

Chaumillon, E., Proust, J.-N., Menier, D., Weber, N., 2008. Incised-valley morphologies and sedimentary-fills within the inner shelf of the Bay of Biscay (France): A synthesis. Journal of Marine Systems 72, 383-396.

718 Chaumillon, E., Tessier, B., Reynaud, J.Y., 2010. Stratigraphic records and variability of incised
719 valleys and estuaries along French coasts. Bulletin de la Société Géologique de France 181,
720 75-85.
721 Clark, J., X. Mitrovica, J., and Alder, J., 2014. Coastal paleogeography of the California-Oregon-
722 Washington and Bering Sea continental shelves during the latest Pleistocene and
723 Holocene: Implications for the archaeological record. Journal of Archaeological Science 52,
724 12–23, doi:10.1016/j.jas.2014.07.030.
725 Clarke, S.H., Field, M.E., and Hirozawa, C.A., 1985. Reconnaissance Geology and Geologic
726 Hazards of the Offshore Coos Bay Basin, Oregon. U.S. Geological Survey Bulletin 1645, 41
727 p.
728 Cohen, J.K., Stockwell Jr., J.W., 1999. CWP/SU: Seismic Unix Release 33: a Free Package for
729 Seismic Research and Processing. Center for Wave Phenomena, Colorado School of Mines.
730 Crockett, J.S., Nittrouer, C.A., Ogston, A.S., Naar, D.F., Donahue, B.T., 2008. Morphology and
731 filling of incised submarine valleys on the continental shelf near the mouth of the Fly
732 River, Gulf of Papua. Journal of Geophysical Research: Earth Surface 113.
733 Dalrymple, R.W., 2006. Incised valleys in time and space: introduction to the volume and an
734 examination of the controls on valley formation and filling. In: Dalrymple, R.W., Leckie,
735 D.A., Tillman, R. (Eds.), Incised Valleys in Time and Space. SEPM Special Publication 85, 5–
736 12.
737 Danforth, W. W., 1997. Xsonar/ShowImage, a complete system for rapid sidescan sonar
738 processing and display (No. 97-686). US Dept. of the Interior, US Geological Survey.

739 Davis, L.G., Punke, M.L., Hall, R.L., Fillmore, M., and Willis, S.C., 2004. Evidence for Late
740 Pleistocene Occupation on the Southern Northwest Coast: Journal of Field Archaeology
741 29, no. 1, 7–16.
742 Davis, Loren G., Steven A. Jenevein, Michele L. Punke, Jay S. Noller, Julia A. Jones, and Samuel C.
743 Willis, 2009. Geoarchaeological Themes in a Dynamic Coastal Environment, Lincoln and
744 Lane Counties, Oregon. In, J.E. O'Connor, R.J. Dorsey, and I.P. Madin, pp. 319-336,
745 Volcanoes to Vineyards: Geologic Field Trips through the Dynamic Landscape of the
746 Pacific Northwest. Geological Society of America Field Trip Guide 15. Geological Society
747 of America, Boulder, Colorado.
748 Davis, Loren G., David B. Madsen, Lorena Becerra-Valdivia, Thomas Higham, David A. Sisson,
749 Sarah M. Skinner, Daniel Stueber, Alexander J. Nyers, Amanda Keen-Zebert, Christina
750 Neudorf, Melissa Cheyney, Masami Izuho, Fumie Iizuka, Samuel R. Burns, Clinton W. Epps,
751 Samuel C. Willis, Ian Buvit, 2019. Late Upper Paleolithic Occupation at Cooper's Ferry,
752 Idaho, USA, ~16,000 Years Ago. Science 365, 891–897.
753 DeMets, C., Gordon, R.G., Argus, D.F., Stein, S., 1990. Current plate motions. Geophysical
754 Journal International 101, 425-478.
755 Dillehay, T.D., Ramirez, C., Pino, M., Collins, M.B., Rossen, J. and Pino-Navarro, J.D., 2008.
756 Monte Verde: seaweed, food, medicine, and the peopling of South America. Science 320,
757 784-786.
758 Erlandson, J.M., 2002. Anatomically modern humans, maritime voyaging, and the Pleistocene
759 colonization of the Americas. The first Americans: the Pleistocene colonization of the New
760 World 27, 59-92.

761 Erlandson, J.M., Graham, M.H., Bourque, B.J., Corbett, D., Estes, J.A. and Steneck, R.S., 2007.
762 The kelp highway hypothesis: marine ecology, the coastal migration theory, and the
763 peopling of the Americas. The Journal of Island and Coastal Archaeology 2(2), 161-174.
764 Fagundes, N.J., Kanitz, R., Eckert, R., Valls, A.C., Bogo, M.R., Salzano, F.M., Smith, D.G., Silva Jr,
765 W.A., Zago, M.A., Ribeiro-dos-Santos, A.K. and Santos, S.E., 2008. Mitochondrial
766 population genomics supports a single pre-Clovis origin with a coastal route for the
767 peopling of the Americas. The American Journal of Human Genetics 82(3), 583-592.
768 Fedje, D., Mackie, Q., Heaton, T., Dixon, E., 2004. Late Wisconsin Environments and
769 Archaeological Visibility on the Northern Northwest Coast. In, Entering America:
770 Northeast Asia and Beringia Before the Last Glacial Maximum, edited by David B. Madsen,
771 University of Utah Press, 97-138.
772 Foyle, A.M. and Oertel, G.F., 1997. Seismic stratigraphy and coastal drainage patterns in the
773 Quaternary section of the southern Delmarva Peninsula, Virginia, USA. Sed. Geol. 80, 261-
774 277.
775 Gobo, K., Ghinassi, M., Nemec, W. and Sjursen, E., 2014. Development of an incised valley-fill at
776 an evolving rift margin: Pleistocene eustasy and tectonics on the southern side of the Gulf
777 of Corinth, Greece. Sedimentology 61, 1086-1119.
778 Goldfinger, C., Nelson, C.H., Morey, A.E., Johnson, J.E., Patton, J.R., Karabanov, E.B., Gutierrez-
779 Pastor, J., Eriksson, A.T., Gràcia, E., Dunhill, G. and Enkin, R.J., 2012. Turbidite event
780 history--Methods and implications for Holocene paleoseismicity of the Cascadia
781 subduction zone. No. 1661-F. US Geological Survey.

782 Goldfinger, C., Henkel, S., Romsos, C., Havron, A., and Black, B., 2014, Benthic Habitat
783 Characterization Offshore the Pacific Northwest, Volume 1: Evaluation of Continental
784 Shelf Geology OCS Study BOEM, 662, 1-161. doi:10.13140/2.1.3345.0561.
785 Green, A. N., Dladla, N., & Garlick, G. L., 2013. Spatial and temporal variations in incised valley
786 systems from the Durban continental shelf, KwaZulu-Natal, South Africa. Marine Geology,
787 335, 148-161. Doi: 10.1016/j.margeo.2012.11.002
788 Green, A. N., Cooper, J. A. G., & Salzmann, L., 2018. The role of shelf morphology and
789 antecedent setting in the preservation of palaeo-shoreline (beachrock and aeolianite)
790 sequences: the SE African shelf. Geo-Marine Letters, 38(1), 5-18. doi: 10.1007/s00367-
791 017-0512-8
792 Gusick, A.E. and J.M. Erlandson. 2019. Paleocoastal Landscapes, Marginality, and Initial
793 Settlement of California's Islands. In, An Archaeology of Abundance: Re-evaluating the
794 Marginality of California's Islands, edited by K. Gill, J. Erlandson, and M. Fauvelle.
795 University of Florida Press, Gainesville. 59-97.
796 Gusick, A.E. and M.K. Faught. 2011. Prehistoric Archaeology Underwater: A Nascent
797 Subdiscipline Critical to Understanding Early Coastal Occupations and Migration Routes.
798 In, Trekking the Shore, edited by N. Bicho, J. Haws, L.G. Davis. Springer, New York, NY, 27-
799 50.
800 Henkart, P., 2006. SIOSEIS. http://sioseis.ucsd.edu.
801 Hill, J. C. and Driscoll, N. W., 2008. Paleodrainage on the Chukchi shelf reveals sea level
802 history and meltwater discharge. Marine Geology 254, 129-151.

803 Hill, J. C., Driscoll, N. W., Brigham-Grette, J., Donnelly, J. P., Gayes, P. T. and Keigwin, L.,
804 2007. New evidence for high discharge to the Chukchi shelf since the Last Glacial
805 Maximum. Quaternary Research 68, 271-279.
806 Holbrook, J. M. and Bhattacharya, J. P., 2012. Reappraisal of the sequence boundary in time and
807 space: Case and considerations for an SU (subaerial unconformity) that is not a sediment
808 bypass surface, a time barrier, or an unconformity: Earth-Science Reviews 113, 271-302.
809 Ishihara, T., Sugai, T. and Hachinohe, S., 2012. Fluvial response to sea-level changes since the
810 latest Pleistocene in the near-coastal lowland, central Kanto Plain, Japan. Geomorphology
811 147-148, 49-60.
812 Ishihara, T. and Sugai, T., 2017. Eustatic and regional tectonic controls on late Pleistocene
813 paleovalley morphology in the central Kanto Plain, Japan. Quatern. Int. 456, 69-84.
814 Jefferson, Anne, Grant, G.E., Lewis, S.L., and Lancaster, S.T., 2010. Coevolution of hydrology and
815 topography on a basalt landscape in the Oregon Cascade Range, USA: Earth Surface
816 Processes and Landforms 35, 803–816, doi: 10.1002/esp.1976.
817 Kelsey, H.M., Bockheim, J.G., 1994. Coastal landscape evolution as a function of eustasy and
818 surface uplift rate, Cascadia margin, southern Oregon. Geological Society of America
819 Bulletin 106, 840-854.
820 Kelsey, H.M., Ticknor, R.L., Bockheim, J.G., and Mitchell, C.E., 1996. Quaternary upper plate
821 deformation in coastal Oregon: Geo- logical Society of America Bulletin 108, 843–860, doi:
822 10.1130/0016-7606(1996)108<0843:QUPDIC>2.3.CO;2.

823 Klotsko, S. and Driscoll, N., 2018. Geomorphological and stratigraphic evidence along the
824 northeastern US margin for Laurentide glacial lake outburst floods during the MIS 2
825 deglaciation. Quaternary Research 90, 139-152.
826 Kulm, L. D., Prince, R. A., and Snavely, P. D., Jr., 1973. Site survey of the northern Oregon
827 continental margin and Astoria fan: Deep Sea Drilling Project Initial Reports 18, 979-986.
828 Lague, D., 2014. The stream power river incision model: evidence, theory and beyond. Earth
829 Surface Processes and Landforms 39, 38-61.
830 Lamb, M.P., Finnegan, N.J., Scheingross, J.S. and Sklar, L.S., 2015. New insights into the
831 mechanics of fluvial bedrock erosion through flume experiments and
832 theory. Geomorphology 244, 33-55.
833 Labaune, C., Tesson, M., Gensous, B., Parize, O., Imbert, P., & Delhaye-Prat, V., 2010. Detailed
834 architecture of a compound incised valley system and correlation with forced regressive
835 wedges: Example of Late Quaternary Têt and Agly rivers, western Gulf of Lions,
836 Mediterranean Sea, France. *Sedimentary Geology*, *223*(3-4), 360-379.
837 https://doi.org/10.1016/j.sedgeo.2009.12.001
838 Laws, A. W., Maloney, J. M., Klotsko, S., Gusick, A. E., Braje, T. J., & Ball, D., 2020. Submerged
839 paleoshoreline mapping using high-resolution Chirp sub-bottom data, Northern Channel
840 Islands platform, California, USA. Quaternary Research, 93(1), 1-22.
841 Liu, Y., Shi, Z., Wang, B., Yu, T., 2018. GPR impedance inversion for imaging and characterization
842 of buried archaeological remains: A case study at Mudu city cite in Suzhou, China. Journal
843 of Applied Geophysics 148, 226-233.

844 Lobo, F.J., García, M., Luján, M., Mendes, I., Reguera, M.I. and Van Rooij, D., 2018. Morphology
845 of the last subaerial unconformity on a shelf: insights into transgressive ravinement and
846 incised valley occurrence in the Gulf of Cádiz. Geo-Marine Letters, 38(1), pp.33-45.
847 Mandryk, C.A., Josenhans, H., Fedje, D.W. and Mathewes, R.W., 2001. Late Quaternary
848 paleoenvironments of Northwestern North America: implications for inland versus coastal
849 migration routes. Quaternary Science Reviews 20, 301-314.
850 Maselli, V., Trincardi, F., 2013. Large-scale single incised valley from a small catchment basin on
851 the western Adriatic margin (central Mediterranean Sea). Global and Planetary Change
852 100, 245-262.
853 Mattheus, C.R., Rodriguez, A.B., Greene, D.L., Jr., Simms, A.R., Anderson, J.B., 2007. Control of
854 Upstream Variables on Incised-Valley Dimension. Journal of Sedimentary Research 77,
855 213-224.
856 Mattheus, C. R. and Rodriguez, A. B., 2011. Controls on late Quaternary incised-valley
857 dimension along passive margins evaluated using empirical data. Sedimentology 58, 1113-
858 1137.
859 McClung, W. S., Cuffey, C. A., Eriksson, K. A., & Terry Jr, D. O., 2016. An incised valley fill and
860 lowstand wedges in the Upper Devonian Foreknobs Formation, central Appalachian Basin:
861 Implications for Famennian glacioeustasy. Palaeogeography, Palaeoclimatology,
862 Palaeoecology, 446, 125-143. doi: 10.1016/j.palaeo.2016.01.014
863 McInelly, G.W., Kelsey, H.M., 1990. Late Quaternary deformation in the Cape Arago-Bandon
864 region of coastal Oregon as deduced from wave-cut platforms. J. Geophys. Res. 95, 669-
865 6713. http://dx.doi.org/10.1029/JB095iB05p06699.

McNeill, L.C., Goldfinger, C., Kulm, L.D., and Yeats, R.S., 2000. Tectonics of the Neogene Cascadia forearc basin: Investigations of a deformed late Miocene unconformity: Geological Society of America Bulletin 112, 1209–1224, doi: 10.1130/0016-7606(2000)112<1209: TOTNCF>2.3.CO;2.

Miall, A. D., 2014. Fluvial depositional systems. Berlin: Springer International Publishing, 316 pp.

Milker, Y., Nelson, A.R., Horton, B.P., Engelhart, S.E., Bradley, L.A. and Witter, R.C., 2016. Differences in coastal subsidence in southern Oregon (USA) during at least six prehistoric megathrust earthquakes. Quaternary Science Reviews 142, 143-163.

Miller MM, Johnson DL, Rubin CM, Dragert H, Wang CY, Qamar A, Goldfinger C., 2001. GPS-determination of along-strike variation in Cascadia margin kinematics: Implications for relative plate motion, subduction zone coupling, and permanent deformation. Tectonics 20, 61–176.

Milliman, J.D. and Syvitsky, J.P.M., 1992. Geomorphic/tectonic control of sediment discharge to the ocean: the importance of small mountainous rivers: Journal of Geology 100, 525-544.

Minor, R., and Toepel, K., 1986. The Archaeology of the Tahkenitch Landing Site: Early Prehistoric Occupation on the Oregon Coast. Heritage Research Associates Report 46 on-file at Oregon State Historic Preservation Office, Salem.

Monteleone, K., Dixon, E. J., and Wickert, A. D., 2013. Lost Worlds: A predictive model to locate submerged archaeological sites in SE Alaska, USA, in: Archaeology in the Digital Era: Papers from the 40th Annual Conference of Computer Applications and Quantitative Methods in Archaeology (CAA), Southampton, 26–29 March 2012, edited by: Earl, G., Sly,

887 T., Chrysanthi, A., Murrieta-Flores, P., Papadopoulos, C., Romanowska, I., and Wheatley,
888 D., 1–12, Amsterdam University Press, Southampton, UK.
889 Muhs, D.R., Kelsey, H.M., Miller, G.H., Kennedy, G.L., Whelan, J.F., and McInelly, G.W., 1990.
890 Age estimates and uplift rates for Late Pleistocene marine terraces—Southern Oregon
891 portion of the Cascadia Forearc: Journal of Geophysical Research 95, 6685–6698, doi:
892 10.1029/JB095iB05p06685.
893 Naish, T. R., and Kamp, P. J. J., 1997. Sequence stratigraphy of sixth order (41 ky) Pliocene-
894 Pleistocene cyclothems, Wanganui basin, New Zealand: A case for the regressive systems
895 tract. Geological Society of America Bulletin 109, 978–999.
896 National Geophysical Data Center, 2003a. U.S. Coastal Relief Model - Central Pacific. National
897 Geophysical Data Center, NOAA. doi:10.7289/V50Z7152 [Accessed February 2018].
898 National Geophysical Data Center, 2003b. U.S. Coastal Relief Model - Northwest Pacific.
899 National Geophysical Data Center, NOAA. doi:10.7289/V5H12ZXJ. [Accessed February
900 2018].
901 NOAA National Centers for Environmental information, Climate at a Glance: Divisional Time
902 Series, published July 2020, retrieved on July 24, 2020
903 from https://www.ncdc.noaa.gov/cag/
904 Nordfjord, S., Goff, J. A., Austin, J. A. and Gulick, S. P. S., 2006. Seismic Facies of Incised-Valley
905 Fills, New Jersey Continental Shelf: Implications for Erosion and Preservation Processes
906 Acting During Latest Pleistocene-Holocene Transgression. Journal of Sed. Research 76,
907 1284- 1303.

O'Connor, J.E., Mangano, J.F., Anderson, S.W., Wallick, J.R., Jones, K.L. and Keith, M.K., 2014. Geologic and physiographic controls on bed-material yield, transport, and channel morphology for alluvial and bedrock rivers, western Oregon. GSA Bulletin 126, 377-397.

Pacific Northwest Hydrography Framework (PNWHF) and the US Geological Survey (USGS). Watershed Boundary Dataset layer for Oregon and Washington. <https://www.pnwhf.org/water-bound-dataset.aspx> Accessed December 2020.

Paola, C., Heller, P.L. and Angevine, C.L., 1992. The large-scale dynamics of grain-size variation in alluvial basins, 1: Theory. Basin Res. 4, 73-90.

Peterson, C.P., Kuhn, L.D., and Gray, J.J., 1986. Geologic map of the ocean floor off Oregon and the adjacent continental margin. Oregon Department of Geology and Mineral Industries, Geologic Map Series 42.

Phillips, J. D., 2011. Drainage area and incised valley fills in Texas rivers: A potential explanation. Sed. Geol. 242, 65-70.

Plink-Björklund, P. and Steel, R.J., 2004. Initiation of turbidity currents: outcrop evidence for Eocene hyperpycnal flow turbidites. Sedimentary Geology 165, 29-52.

Pojar, J., Klinka, K., and Demarchi, D.A., 1991. Coastal Western Hemlock Zone. In Meidinger D, Pojar J (eds) Ecosystems of British Columbia. BC Special Report Series No 6, Victoria: BC Ministry of Forests, 95–111.

Posamentier, H. W., and Vail, P.R., 1988. Eustatic controls on clastic deposition II—Sequence and systems tract models, in Sea-Level Changes: An Integrated Approach, edited by C. K. Wilgus et al., Spec. Publ. Soc. Econ. Paleontol. Mineral. 42, p. 125 – 154.

929 Posamentier, H.W., Allen, G.P., James, D.P., Tesson, M, 1992. Forced Regressions in a Sequence
930 Stratigraphic Framework: Concepts, Examples and Exploration Significance, AAPG Bulletin
931 76, 1687-1709.
932 Posamentier, H.W. and Allen, G.P., 1993. Siliclastic sequence stratigraphic patterns in foreland
933 ramp-type basins: Journal of Geology 21, 455-458.
934 Posamentier, H.W., 2001. Lowstand alluvial bypass systems: incised vs. unincised. AAPG Bulletin
935 85, 1771 – 1793.
936 Pretorius, L., Green, A. N., Cooper, J. A. G., Hahn, A., & Zabel, M., 2019. Outer-to inner-shelf
937 response to stepped sea-level rise: Insights from incised valleys and submerged
938 shorelines. Marine Geology, 416, 105979. doi: 10.1016/j.margeo.2019.105979
939 Punke, Michele L. and Loren G. Davis, 2006. Problems and Prospects in the Preservation of Late
940 Pleistocene Cultural Sites in Southern Oregon Coastal River Valleys: Implications for
941 Evaluating Coastal Migration Routes. Geoarchaeology: An International Journal 21, 333-
942 350.
943 Reeder-Myers, L., Erlandson, J.M., Muhs, D.R., Rick, T.C., 2015. Sea level, paleogeography, and
944 archeology on California's Northern Channel Islands. Quaternary Research 83, 263-272.
945 Ruddiman, W.F., 2013. Tectonic uplift and climate change. Springer Science & Business Media.
946 Salzmann, L., Green, A., & Cooper, J. A. G., 2013. Submerged barrier shoreline sequences on a
947 high energy, steep and narrow shelf. Marine Geology, 346, 366-374. doi:
948 10.1016/j.margeo.2013.10.003

Santra, M., Steel, R., and Olariu, C., and Sweet, M., 2013. Stages of sedimentary prism development on a convergent margin — Eocene Tyee Forearc Basin, Coast Range, Oregon, USA. Global and Planetary Change 103, 207-231, doi:10.1016/j.gloplacha.2012.11.006.

Scheingross, J.S., Brun, F., Lo, D.Y., Omerdin, K., Lamb, M.P., 2014. Experimental evidence for fluvial bedrock incision by suspended and bedload sediment. Geology 42, 523-526.

Schumm, S. A., 1993, River response to baselevel change: Implications for sequence stratigraphy. Journal of Geology 101, 279 – 294.

Schumm, S.A., Harvey, M.D. and Watson, C.C., 1984. Incised Channels: Morphology, Dynamics and Control. Water Resources Publication, Chelsea, MI, 200 pp.

Seely, D.R., Vail, P.R., and Walton, G.G., 1974. Trench slope model, in Burk, C.A., and Drake, C.L., eds., The Geology of Continental Margins: New York, Springer-Verlag, 249–260.

Simms, A.R., Anderson, J.B., Taha, Z.P. and Rodriguez, A.B., 2006. Over–filled versus under-filled incised valleys: lessons from the Quaternary Gulf of Mexico. In, Incised Valleys Through Space and Time, Eds R. Dalrymple, D. Leckie and R. Tillman, SEPM Special Publication 85, 117–139.

Simms, A. & Rouby, H. & Lambeck, K., 2016. Marine terraces and rates of vertical tectonic motion: The importance of glacio-isostatic adjustment along the Pacific coast of central North America: Geological Society of America Bulletin 128, 81-93, doi:10.1130/B31299.1.

Siuslaw Basin Council and Ecotrust, January 2002. A watershed assessment for the Siuslaw Basin. Archived at < https://nrimp.dfw.state.or.us/DataClearinghouse/default.aspx?p=202&XMLname=73.xml > from <http://www.inforain.org/siuslaw/>, accessed March 15, 2020.

971 Sklar, L.S., Dietrich, W.E., 2001. Sediment and rock strength controls on river incision into
972 bedrock. Geology 29, 1087–1090. https://doi.org/10.1130/0091-
973 7613(2001)029<1087:SARSCO>2.0.CO;2
974 Snavely Jr, P. D., 1987. Tertiary geologic framework, neotectonics, and petroleum potential of
975 the Oregon-Washington continental margin.
976 Snavely, P.D., Pearl, J.E., Lander, D.L. and Scott, E.W., 1977. Interim report on petroleum
977 resources potential and geologic hazards in the outer continental shelf: Oregon and
978 Washington Tertiary province, U.S. Geological Survey Open-File Report No. 77-282, 64 p.
979 Snavely, P. D. and E. M. Baldwin, 1948. Siletz River Volcanic Series, Northwestern
980 Oregon. *AAPG Bulletin* 32, 806–812. doi: https://doi.org/10.1306/3D933B78-16B1-11D7-
981 8645000102C1865D.
982 Snavely, P. D., Jr., Wagner, H. C., Rau, W. W., and Bukry, David, 1981. Correlation of Tertiary
983 rocks penetrated in wells drilled on the southern Oregon continental margin. U.S.
984 Geological Survey Open-File Report 81-1351, 20 p.
985 Stillwater Sciences, 2000. North Umpqua cooperative watershed analysis. Technical appendix to
986 the synthesis report, Appendix 2–1, Sediment budget for the North Umpqua River basin,
987 Prepared for PacifiCorp, North Umpqua hydroelectric project, FERC Project No. 1927:
988 Portland, Oregon, 113 p.
989 Strong, N. and Paola, C., 2008. Valleys that never were: time surfaces versus stratigraphic
990 surfaces. J. Sed. Res. 78, 579–593.
991 Summerfield, M.A., 1985. Plate tectonics and landscape development on the African continent.
992 In, Tectonic Geomorphology, 27–51.

993 Suter, J. R., and Berryhill, H. L., 1985. Late Quaternary shelf-margin deltas, northwest Gulf of
994 Mexico. AAPG Bulletin 69, 77 – 91.
995 Talling, P. J., 1998. How and where do incised valleys form if sea level remains above the shelf
996 edge? Journal of Geology 26, 87 – 90.
997 Tesson, M., Posamentier, H., Gensous, B., 2015. Compound incised-valley characterization by
998 high-resolution seismics in a wave-dominated setting: Example of the Aude and Orb
999 rivers, Languedoc inner shelf, Gulf of Lion, France. Marine Geology 367, 1-21.
1000 Thieler, E.R., Butman, B., Schwab, W.C., Allison, M.A., Driscoll, N.W., Donnelly, J.P. and Uchupi,
1001 E., 2007. A catastrophic meltwater flood event and the formation of the Hudson Shelf
1002 Valley. Palaeogeography, Palaeoclimatology, Palaeoecology 246, 120-136.
1003 Törnqvist, T.E., Wortman, S.R., Mateo, Z.R.P., Milne, G.A., Swenson, J.B., 2006. Did the last sea
1004 level lowstand always lead to cross-shelf valley formation and source-to-sink sediment
1005 flux? Journal of Geophysical Research: Earth Surface 111, 13 pp.
1006 Twichell, D.C., Cross, V.A. and Peterson, C.D., 2010. Partitioning of sediment on the shelf
1007 offshore of the Columbia River littoral cell. Marine Geology 273, 11–31.
1008 Vail, P. R., Mitchum Jr, R. M., & Thompson III, S., 1977. Seismic stratigraphy and global changes
1009 of sea level, Part 4. Global cycles of relative changes of sea level. In, Seismic stratigraphy
1010 applications to hydrocarbon exploration, ed. C.E. Payton, American Association of
1011 Petroleum Geologists Memoir 26, 83-97.
1012 VanLaningham, S., Meigs, A., Goldfinger, C., 2006. The effects of rock uplift and rock resistance
1013 on river morphology in a subduction zone forearc, Oregon, USA. Earth Surface Processes
1014 and Landforms 31, 1257–1279.

1015 Van Wagoner, J.C., Posamentier, H.W., R.M. Mitchum, Vail, P.R., Sarg, J.F., Loutit, T.S. and
1016 Hardenbol, J., 1988. An overview of sequence stratigraphy and key definitions. In: C.W.,
1017 Wilgus et al., (Eds.), sea level changes: an integrated approach, Society of Economic
1018 Paleontologists and Mineralogists special publication 42, 39- 45.
1019 Vital, H., Furtado, S.F.L. and Gomes, M.P. (2010) Response of the Apodi-Mossoró estuary-
1020 incised valley system (NE Brazil) to sea-level fluctuations. Brazilian journal of
1021 Oceanography, 58, 13-24.
1022 Walker, G.W. and MacLeod, N.S., 1991. Geologic map of Oregon. U.S. Geological Survey, scale
1023 1:500,000.
1024 Wallick, J.R., O'Connor, J.E., Anderson, S., Keith, M., Cannon, C., and Risley, J.C., 2011. Channel
1025 change and bed- material transport in the Umpqua River basin, Oregon. U.S. Geological
1026 Survey Scientific Investigations Report 2011–5041, 112 p.
1027 Wang, R., Colombera, L., Mountney, N.P., Veiga, G., 2019. Geological controls on the geometry
1028 of incised-valley fills: Insights from a global dataset of late-Quaternary examples.
1029 Sedimentology 66, 2134-2168.
1030 Weber, N., Chaumillon, E., Tesson, M., Garlan, T., 2004. Architecture and morphology of the
1031 outer segment of a mixed tide and wave-dominated-incised valley, revealed by HR seismic
1032 reflection profiling: the paleo-Charente River, France. Marine Geology 207, 17-38.
1033 Wells, Ray, David Bukry, Richard Friedman, Doug Pyle, Robert Duncan, Peter Haeussler, Joe
1034 Wooden, 2014. Geologic history of Siletzia, a large igneous province in the Oregon and
1035 Washington Coast Range: Correlation to the geomagnetic polarity time scale and

implications for a long-lived Yellowstone hotspot. *Geosphere* 10, 692–719. doi: https://doi.org/10.1130/GES01018.1

Wells, R.E., Jayko, A., Niem, A.R., Black, G., Wiley, T., Baldwin, E., and Molenaar, K.M., Wheeler, K.L., Givler, R., and DuRoss, C., 2001. Geologic map and database of the Roseburg, Oregon 30' x 60' Quadrangle, Douglas and Coos Counties, Oregon. U.S. Geological Survey Miscellaneous Investigations Map and Open-File Report OF00–376, 55 p., and 2 map sheets, scale 1:100,000.

Weschenfelder, J., Baitelli, R., Corrêa, I.C.S., Bortolin, E.C., dos Santos, C.B., 2014. Quaternary incised valleys in southern Brazil coastal zone. Journal of South American Earth Sciences 55, 83-93.

Wescott, W. A., 1993. Geomorphic thresholds and complex response of fluvial systems—some implications for sequence stratigraphy. AAPG Bulletin 77, 1208-1218.

Wheatcroft, R. A., & Sommerfield, C. K., 2005. River sediment flux and shelf sediment accumulation rates on the Pacific Northwest margin. Continental Shelf Research, 25(3), 311-332. https://doi.org/10.1016/j.csr.2004.10.001

Whipple KX, Tucker GE. 2002. Implications of sediment-flux-dependent river incision models for landscape evolution. Journal of Geophysical Research 107, ETG 3-1-ETG 3-20.

Wilson, K., Berryman, K., Cochran, U. and Little, T., 2007. A Holocene incised valley infill sequence developed on a tectonically active coast: Pakarae River, New Zealand. Sed. Geol. 197, 333-354.

1056 Witter, R.C., Kelsey, H.M., Hemphill-Haley, E., 2003. Great Cascadia earthquakes and tsunamis
1057 of the past 6700 years, Coquille River estuary, southern coastal Oregon. Geological Society
1058 of America Bulletin 115, 1289-1306. http://dx.doi.org/10.1130/B25189.1.
1059 Woolfe, K.J., Larcombe, P., Naish, T. and Purdon, R.G., 1998. Lowstand rivers need not incise the
1060 shelf: an example from the Great Barrier Reef, Australia, with implications for sequence
1061 stratigraphic models. Geology, 26, 75-78.
1062 Worona, M.A., Whitlock, C., 1995. Late Quaternary vegetation and climate history near Little
1063 Lake, central Coast Range, Oregon. GSA Bulletin 107, 867-876.
1064 Zaitlin, B.A., Dalrymple, R.W. and Boyd, R., 1994. The stratigraphic organization of incised-valley
1065 systems associated with relative sea-level change. In: Incised-Valley Systems: Origin and
1066 Sedimentary Sequences (Eds R.W. Dalrymple, R. Boyd and B.A. Zaitlin), SEPM Special
1067 Publication 51, 45–60.
1068 Zecchin, M. and Catuneanu, O., 2013. High-resolution sequence stratigraphy of clastic shelves I:
1069 units and bounding surfaces. Marine and Petroleum Geology 39, 1-25.
1070 Zhang, G.J. and Li, C.X. (1996) The fills and stratigraphic sequences in the Qiantangjiang incised
1071 paleovalley. China. J. Sed. Res. 66, 406–414.
1072

1073 **Figure Captions**

1074 Figure 1. Regional maps of the study location in central Oregon, USA. (A) Overview of the
1075 tectonic regime of the study area. SR = Siuslaw River, UR = Umpqua River, SUR = South Umpqua
1076 River, NUR = North Umpqua River. (B) Overview of the onshore geologic provinces within the
1077 river basins and offshore geology (based on Clarke et al., 1985 and Peterson et al., 1986).

1078 Bathymetric contours are 50 m. The 150 m contour in white is the approximate shelf edge. Js =
1079 late Jurassic sedimentary rocks, Tmc = late Miocene to Pliocene diatomaceous silty claystone,
1080 Tpm = Mio-cene to Pliocene mudstone and siltstone, Tsu = Eocene to Miocene marine
1081 sedimentary rocks with interbedded volcanics, Qtpm = late Miocene to Pleistocene poorly
1082 indurated siltstone and sandstone (Clarke et al., 1985 and Peterson et al., 1986).
1083 Bathymetry/topography data is from NOAA's Coastal Relief Model (NGDC, 2003a; 2003b).
1084 Other GIS datasets from the Oregon Spatial Data Library
1085 (https://spatialdata.oregonexplorer.info/geoportal/).
1086
1087 Figure 2. Trackline map for seismic data used in this study. Lines shown in figures are labeled
1088 and bolded in yellow. Notable geographic features are labeled.
1089
1090 Figure 3. (A)Paleoshorelines since the last glacial maximum with profile locations for B-D
1091 plotted. Paleoshorelines are based on a glacio-isostatic adjusted sea level curve (inset) for the
1092 region (Clark et al., 2014). Labels are the age of the shorelines in thousands of years ago. (B-C)
1093 Percent-slope along profiles of the (B) Siuslaw shelf and (C) Umpqua shelf from the modern
1094 shoreline to 200 mbsl. Onshore slopes (dashed lines) are averages based on full fluvial profiles
1095 shown in Supplementary Figure 1. (D) Slope of mapped paleovalley thalweg. Depths are plotted
1096 at distances along Umpqua shelf profile for comparison of cross-shelf gradient differences.
1097
1098 Figure 4. Maps of regional structure
1099 (http://activetectonics.coas.oregonstate.edu/casc_structure.htm) and features from

1100 geophysical data overlaying background bathymetry in grayscale. Structure reflects different
1101 controls on shelf morphology through time, mainly driven by compression along the Cascadia
1102 subduction zone. SL = Siltcoos Lake, TaL = Tahkenitch Lake, TnL = Tenmile Lake. (A) Regional
1103 structure and backscatter data (SDSU, BOEM, OSU). The backscatter highlights hardgrounds
1104 that have been uplifted due to tectonic motion in the region. Some of the hardgrounds are
1105 oriented in a linear fashion, creating a series of ridges, while others have a more modular
1106 coverage. (B) Map of Umpqua paleovalley fill thickness and location of the ES overlain by the
1107 regional structure. The white line is the 150 m contour, the approximate shelf edge. (C)
1108 Location of mapped hardground based on chirp data with regional structure. Protruding
1109 hardgrounds stick out above the surrounding seafloor where “all hardgrounds” includes those
1110 that came very close to the surface (within 0.015 s TWTT). (D) Map comparing Umpqua
1111 paleovalley fill thickness and protruding hardground locations. Fill thickness thins towards
1112 protruding hardgrounds. Any overlap is a result of the gridding parameters.
1113
1114 Figure 5. Chirp Line 44 with uninterpreted (top) and interpreted (bottom) versions. Three
1115 different expressions of hardgrounds are imaged. Note the difference in paleodrainage valley
1116 character between inner shelf incision and outer shelf scour of preexisting structural low.
1117
1118 Figure 6. Chirp Line 54 with more vertically exaggerated section of outer shelf Umpqua valley
1119 on bottom. This profile captures the most well-defined instance of the outer shelf valley, where
1120 it is located within a syncline. The paleovalley is bounded to the south by a set of uplifted linear
1121 hardgrounds (Fig. 4). Folding and faulted strata are imaged on the northern extent of the

profile. This is associated with a broad shallowing of the seafloor and hardgrounds that protrude above the surrounding seafloor.

Figure 7. Sections of chirp profiles highlighting incision of the inner shelf portion of the Paleo-Umpqua drainage valley.

Figure 8. Chirp Line 13 with uninterpreted (top) and interpreted (bottom) versions. This profile cuts across the northern extent of the paleo-Umpqua drainage system.

Figure 9. Chirp Line 42 with uninterpreted (top) and interpreted (bottom) versions. The outer shelf paleovalley deepens towards the shelf edge along an across-margin anticline.

Figure 10. Chirp Line 48 with uninterpreted (top) and interpreted (bottom) versions. Representative profile showing the extensive structure across the shelf. Anticlines and synclines underlie the seafloor in much of the area. Highs associated with this folding stick out above the surrounding seafloor as protruding hardgrounds.

Figure 11. Knudsen Line 251_0205 with uninterpreted (top) and interpreted (bottom) versions. There is no distinct channel feature offshore from the modern Siuslaw River. There is only a high amplitude, hummocky reflector mapped in the region as the Erosion Surface (ES). Inset highlights the scoured surface of the ES and internal reflectors of the overlying sediments.

1144 Figure 12. Knudsen Line 251_1345 highlighting the absence of stratigraphy on the outer shelf.
1145 The shelf is sediment starved in the vicinity of the Siuslaw River, but a wedge of sediment is
1146 imaged beyond the shelf break.
1147
1148 Figure 13. Fence diagram of the paleodrainage system offshore from the modern Umpqua
1149 River. The drainage valleys are separated by uplifted hardgrounds, that are both, exposed on
1150 the seafloor and buried.
1151
1152

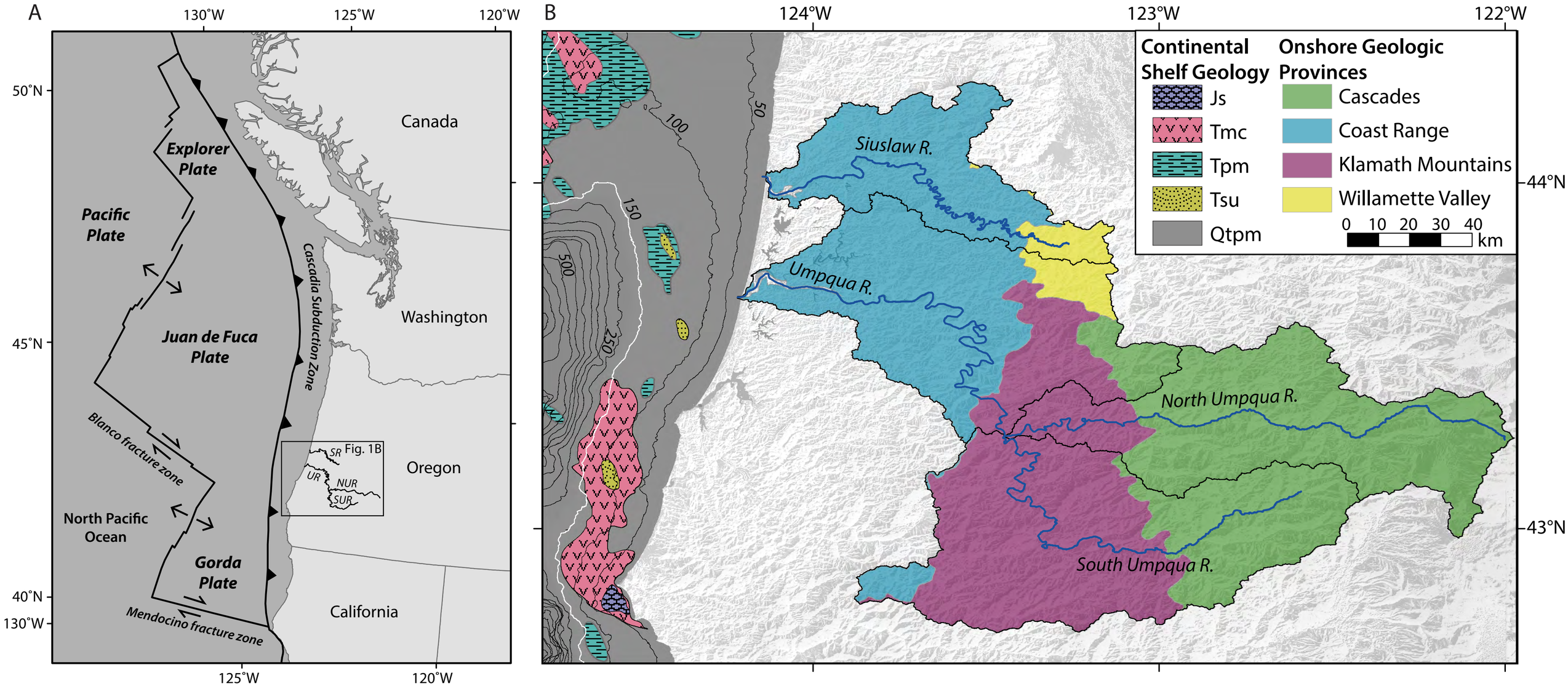
A
130°W
125°W
120°W
50°N
45°N
40°N
130°W
125°W
120°W
Canada
Washington
Oregon
California
Explorer Plate
Pacific Plate
Juan de Fuca Plate
Gorda Plate
North Pacific Ocean
Cascadia Subduction Zone
Blanco fracture zone
Mendocino fracture zone
Fig. 1B
SR
UR
NUR
SUR
B
124°W
123°W
122°W
44°N
43°N
50
100
150
500
250
Siuslaw R.
Umpqua R.
North Umpqua R.
South Umpqua R.
Continental Shelf Geology
Js
Tmc
Tpm
Tsu
Qtpm
Onshore Geologic Provinces
Cascades
Coast Range
Klamath Mountains
Willamette Valley
0 10 20 30 40
km

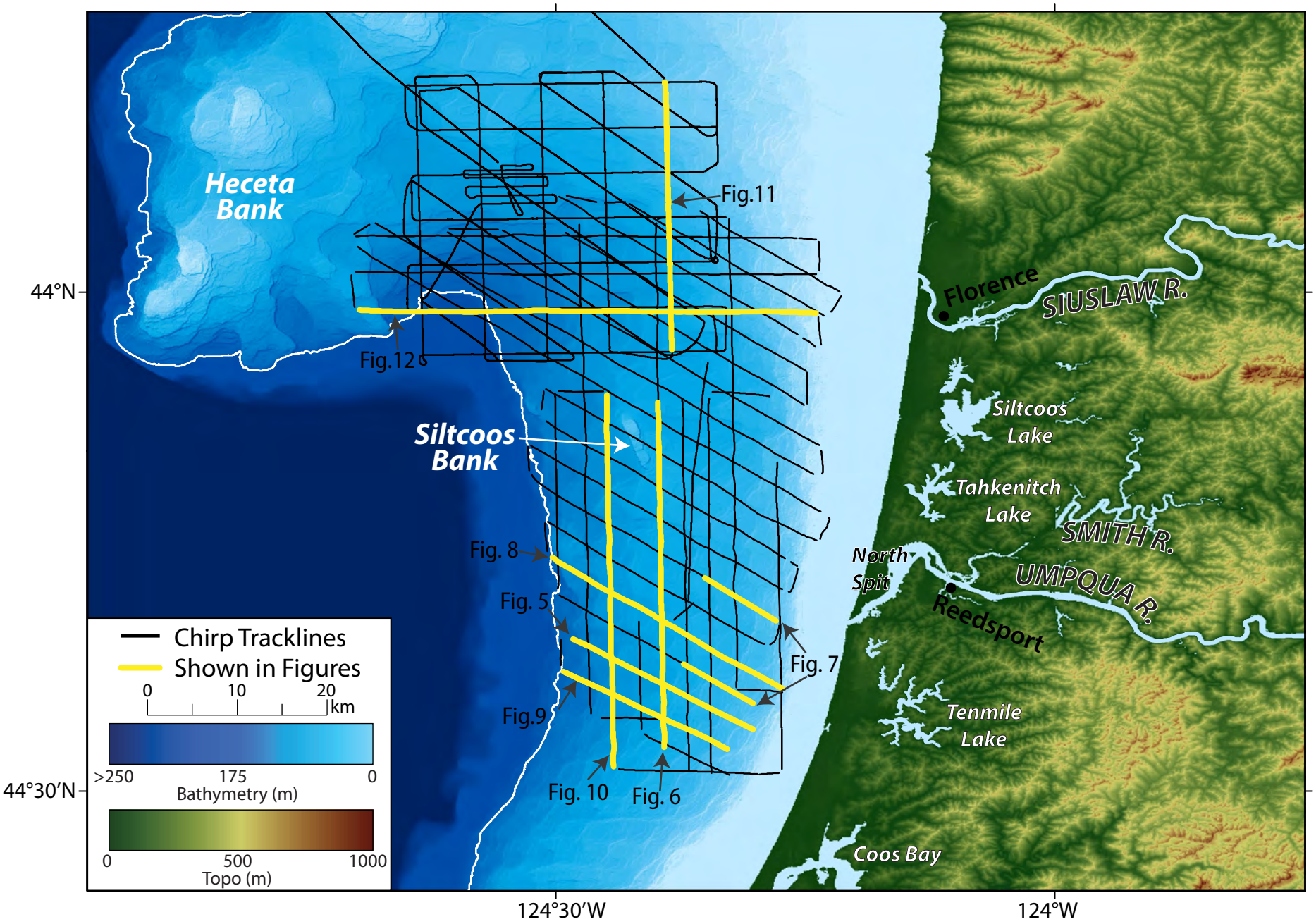
Heceta Bank
Siltcoos Bank
Fig.11
Fig.12
Fig. 8
Fig. 5
Fig. 7
Fig.9
Fig. 10
Fig. 6
Florence
SIUSLAW R.
Siltcoos Lake
Tahkenitch Lake
SMITH R.
North Spit
UMPQUA R.
Reedsport
Tenmile Lake
Coos Bay
Chirp Tracklines
Shown in Figures
0 10 20 km
>250 175 0
Bathymetry (m)
0 500 1000
Topo (m)
44°N
44°30'N
124°30'W
124°W

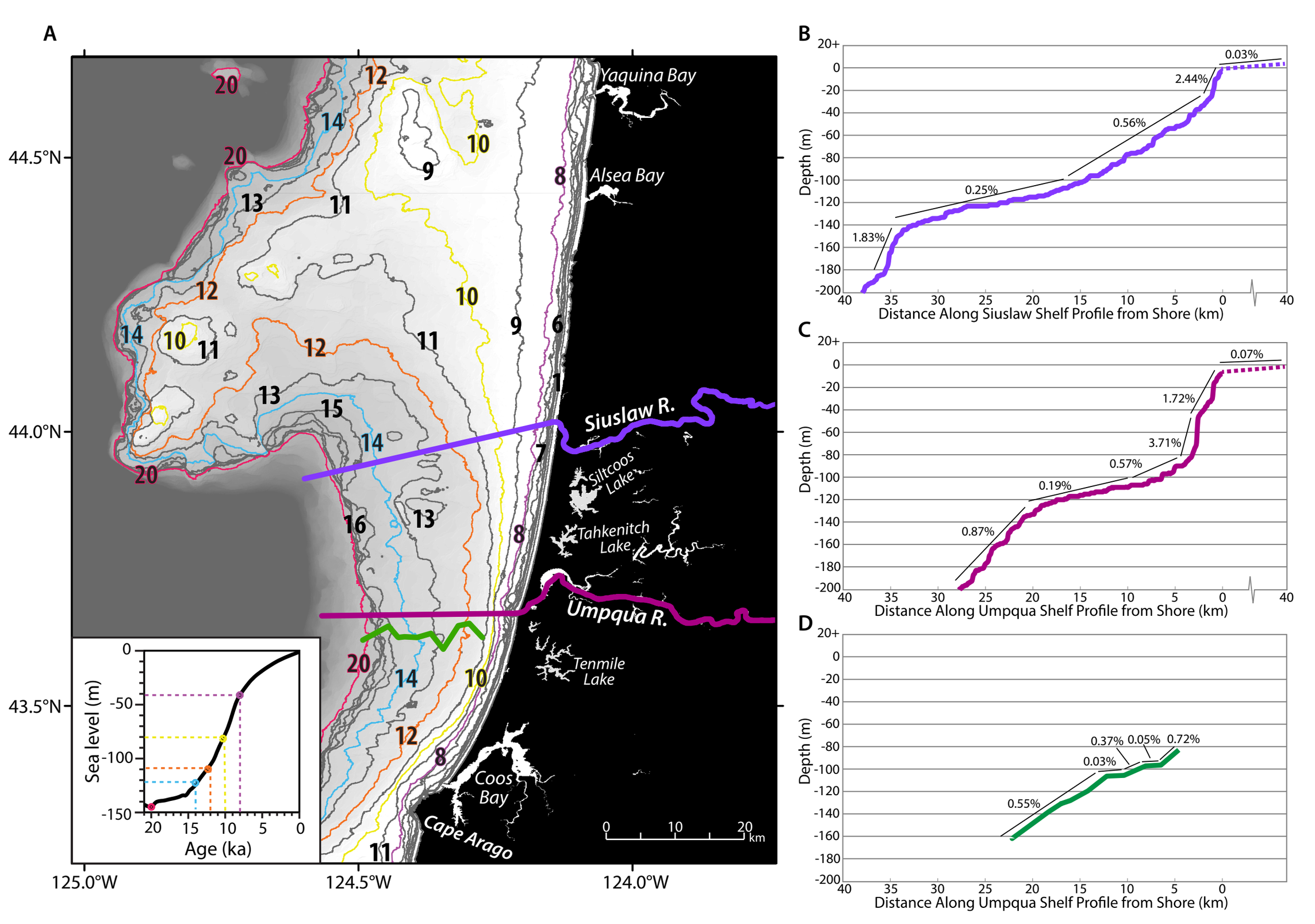
A
B
C
D
Yaquina Bay
Alsea Bay
Siuslaw R.
Siltcoos Lake
Tahkenitch Lake
Umpqua R.
Tenmile Lake
Coos Bay
Cape Arago
44.5°N
44.0°N
43.5°N
125.0°W
124.5°W
124.0°W
0 10 20 km
Sea level (m)
Age (ka)
Depth (m)
Distance Along Siuslaw Shelf Profile from Shore (km)
0.03%
2.44%
0.56%
0.25%
1.83%
Distance Along Umpqua Shelf Profile from Shore (km)
0.07%
1.72%
3.71%
0.57%
0.19%
0.87%
Distance Along Umpqua Shelf Profile from Shore (km)
0.37%
0.05%
0.72%
0.03%
0.55%

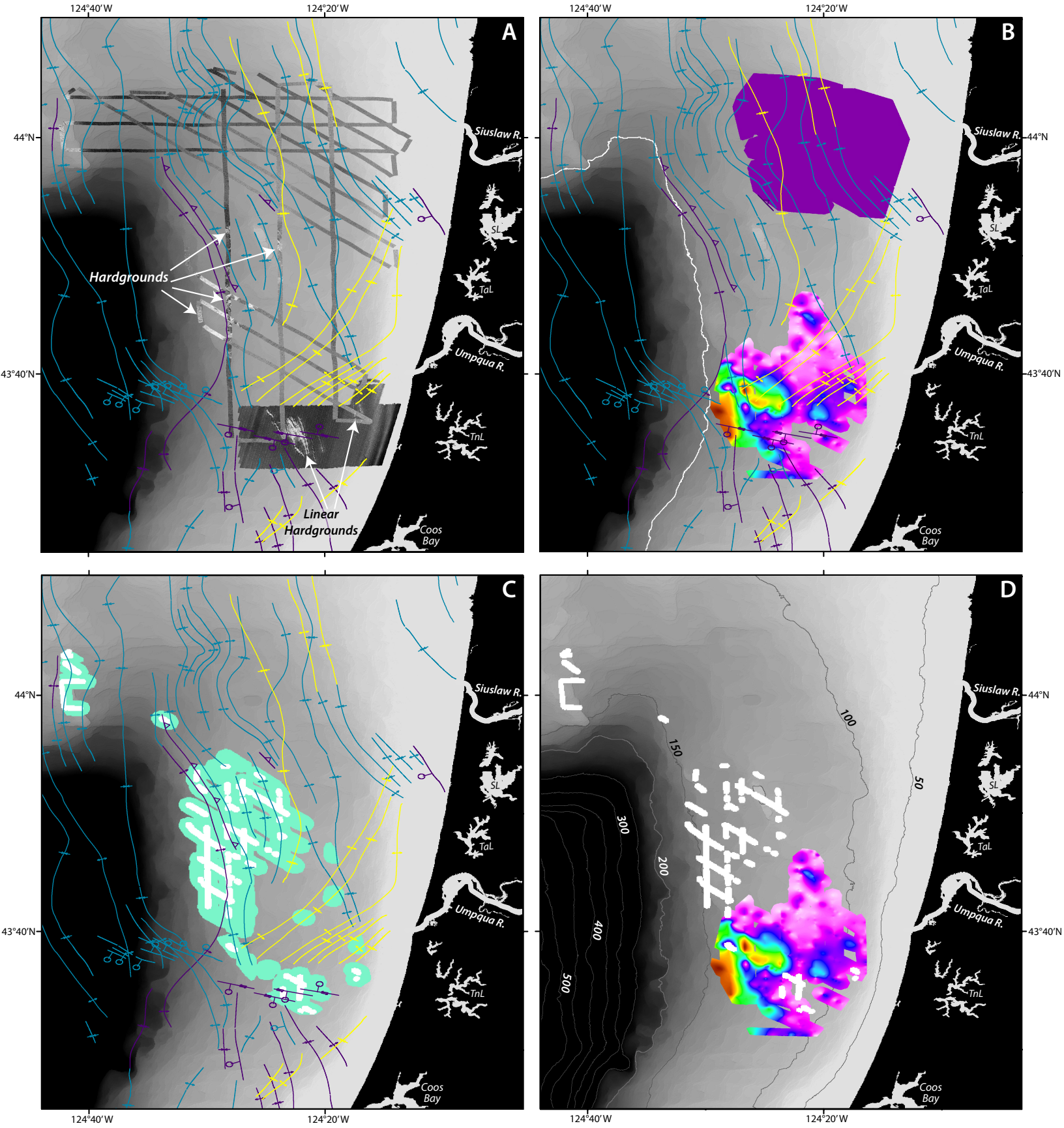
A
B
C
D
124°40′W
124°20′W
44°N
43°40′N
Siuslaw R.
SL
TaL
Umpqua R.
TnL
Coos Bay
Hardgrounds
Linear Hardgrounds
100
150
50
300
200
400
500
0
10
20 km
>250
Background Bathymetry (mbsl)
0
Structure
Active
Pleistocene
Pre-pleistocene
Mapped Features
Erosion Surface (ES)
Protruding Hardgrounds
All Hardgrounds
0
Valley Fill Thickness (m)
25
High
Low
Backscatter

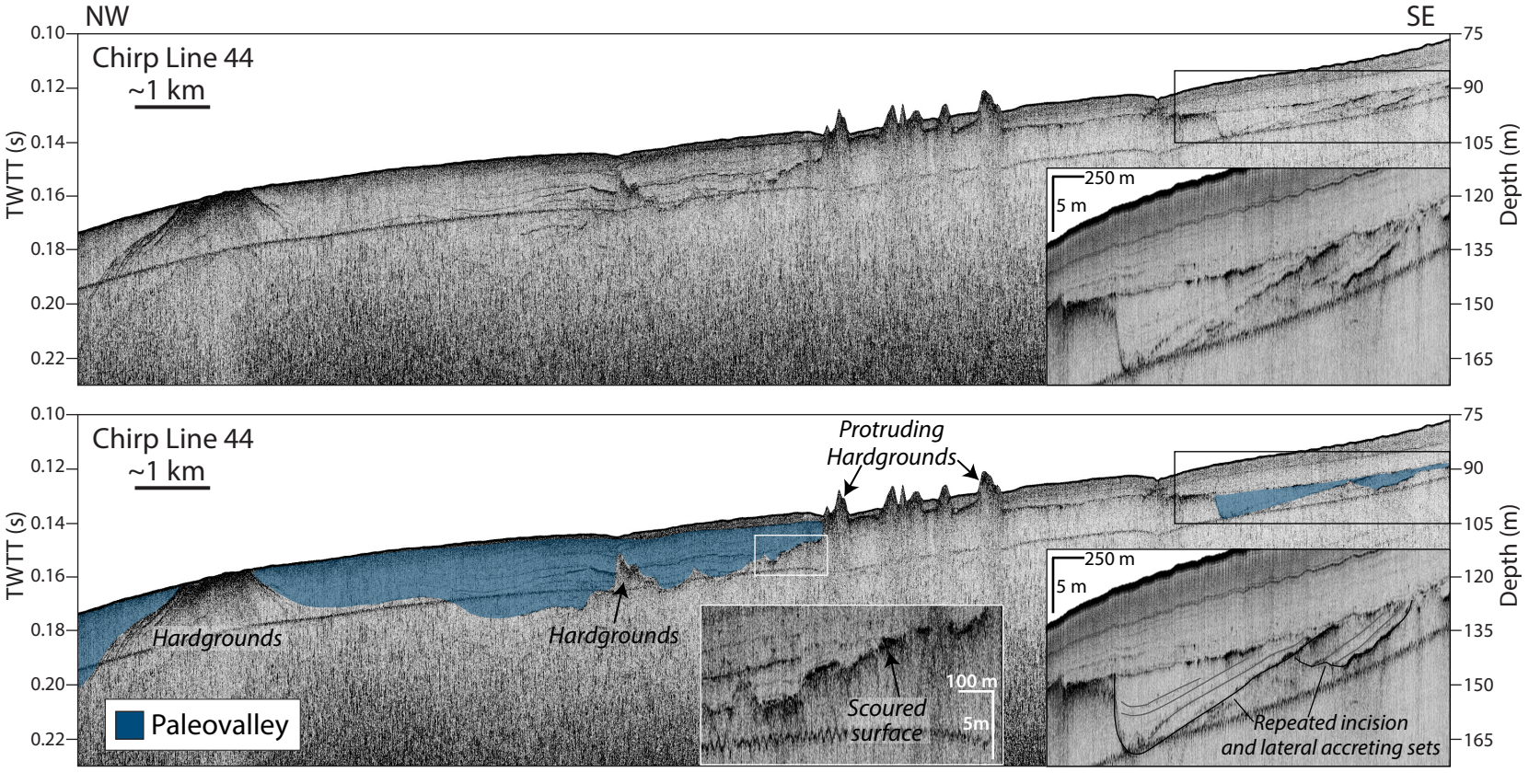
NW
SE
Chirp Line 44
~1 km
TWTT (s)
Depth (m)
0.10
0.12
0.14
0.16
0.18
0.20
0.22
75
90
105
120
135
150
165
250 m
5 m
Chirp Line 44
~1 km
Protruding
Hardgrounds
Hardgrounds
Hardgrounds
Paleovalley
100 m
5m
Scoured
surface
Repeated incision
and lateral accreting sets

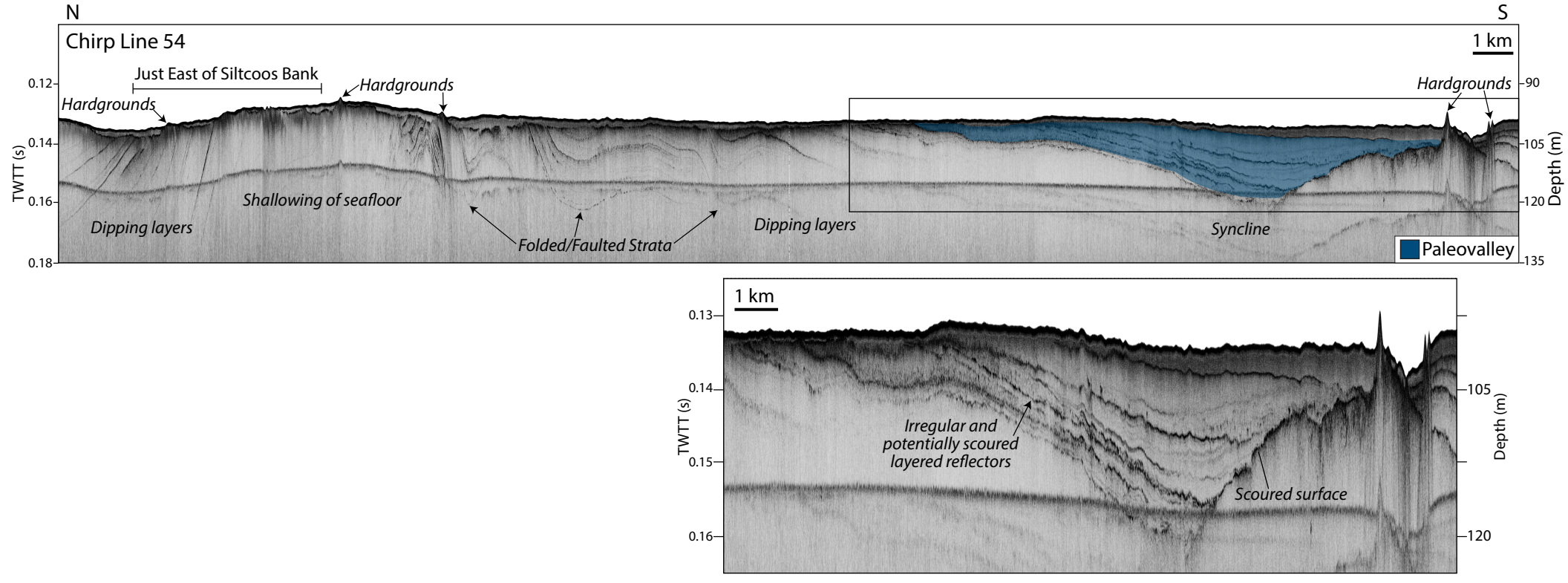
N
S
Chirp Line 54
1 km
Just East of Siltcoos Bank
Hardgrounds
Hardgrounds
Hardgrounds
TWTT (s)
0.12
0.14
0.16
0.18
Depth (m)
90
105
120
135
Shallowing of seafloor
Dipping layers
Folded/Faulted Strata
Dipping layers
Syncline
Paleovalley
1 km
TWTT (s)
0.13
0.14
0.15
0.16
Depth (m)
105
120
Irregular and
potentially scoured
layered reflectors
Scoured surface

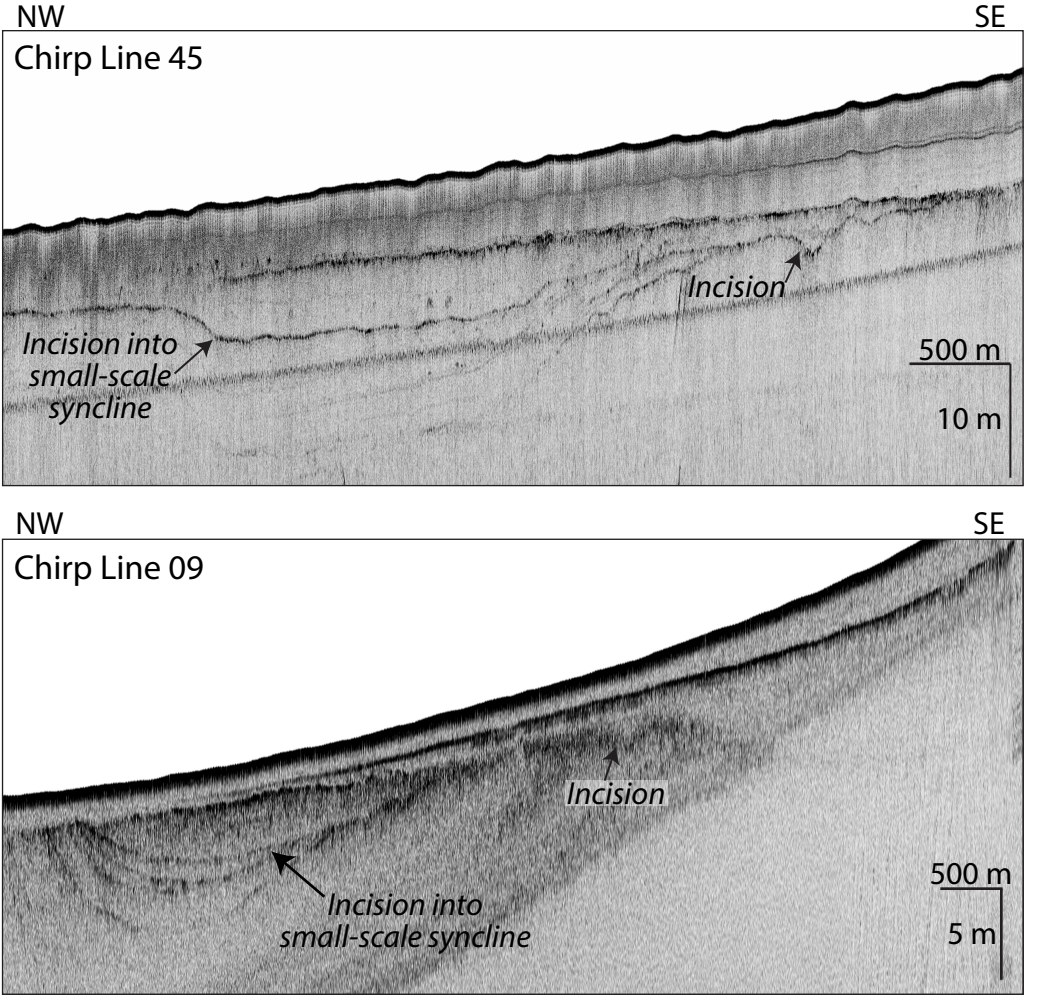
NW
SE
Chirp Line 45
Incision
Incision into
small-scale
syncline
500 m
10 m
NW
SE
Chirp Line 09
Incision
Incision into
small-scale syncline
500 m
5 m

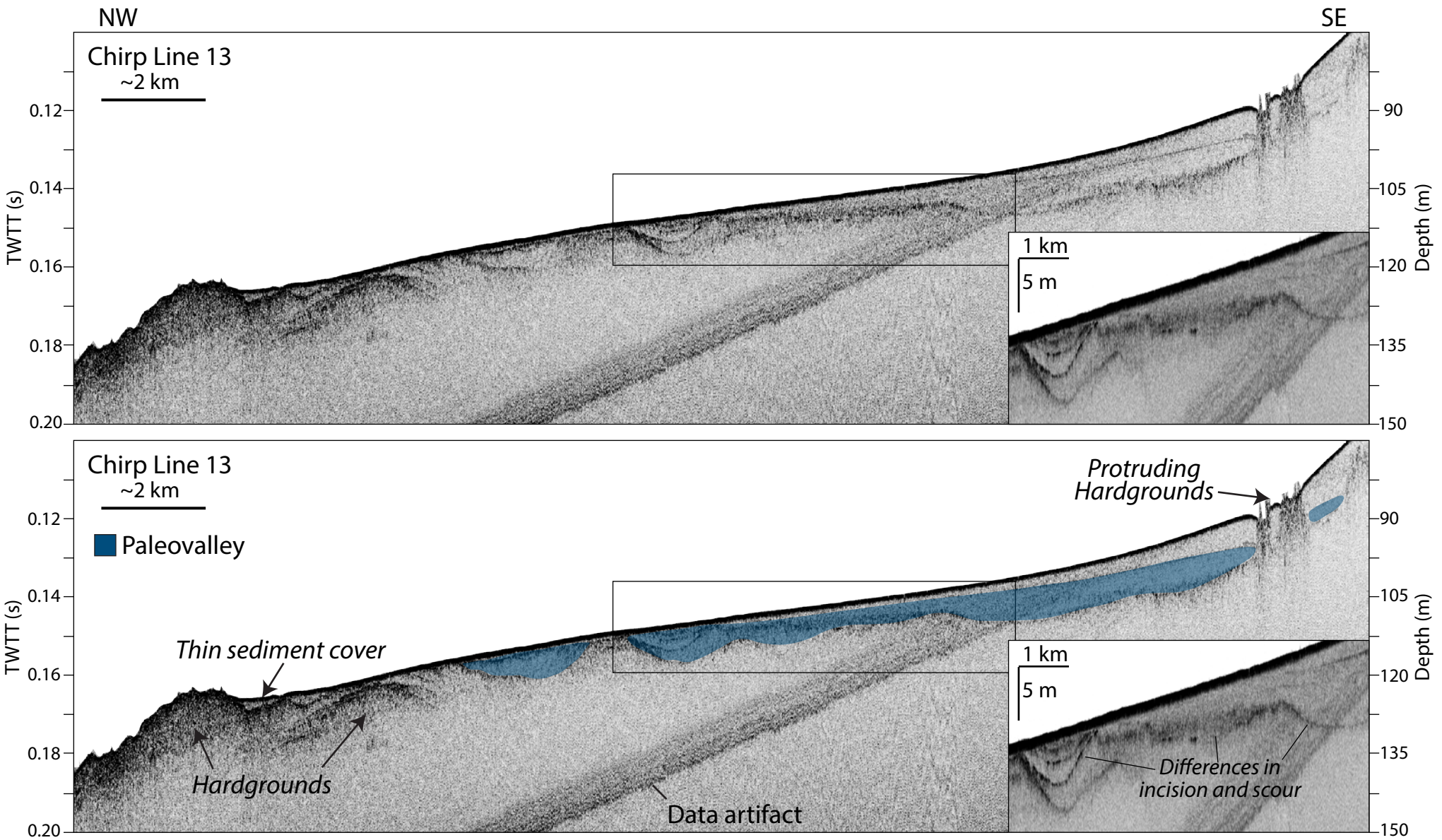
NW
SE
Chirp Line 13
~2 km
TWTT (s)
0.12
0.14
0.16
0.18
0.20
Depth (m)
90
105
120
135
150
1 km
5 m
Chirp Line 13
~2 km
Paleovalley
Protruding Hardgrounds
Thin sediment cover
Hardgrounds
Data artifact
Differences in incision and scour

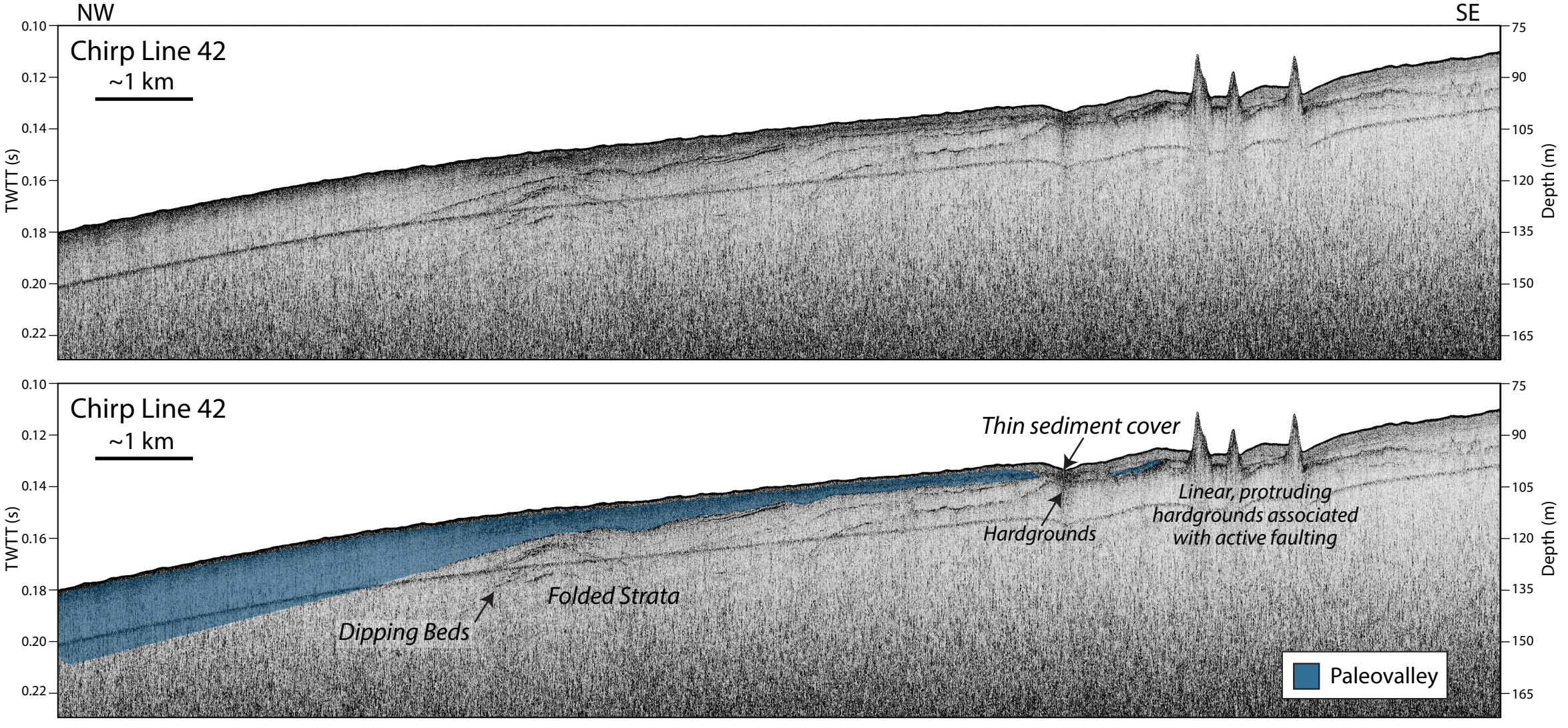
NW
SE
Chirp Line 42
~1 km
TWTT (s)
Depth (m)
0.10
0.12
0.14
0.16
0.18
0.20
0.22
75
90
105
120
135
150
165
Chirp Line 42
~1 km
Thin sediment cover
Hardgrounds
Linear, protruding hardgrounds associated with active faulting
Folded Strata
Dipping Beds
Paleovalley

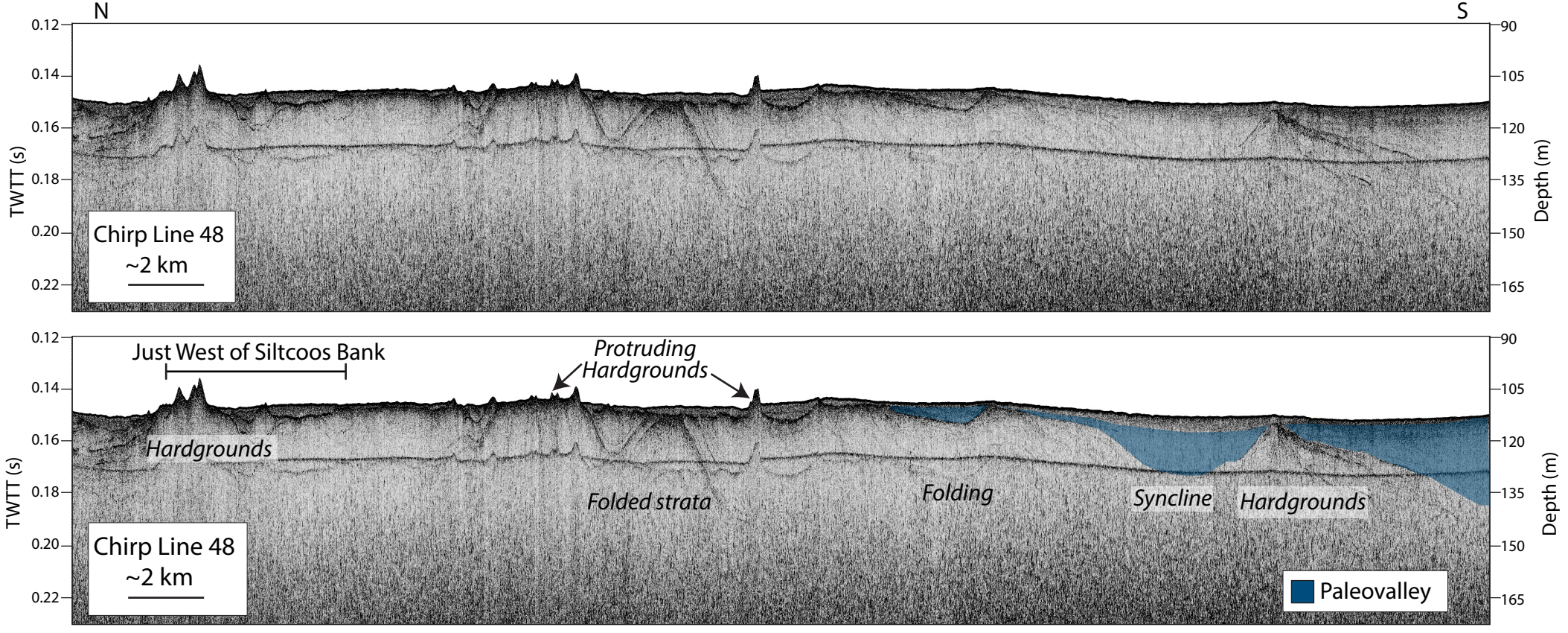
N
S
0.12
0.14
0.16
0.18
0.20
0.22
TWTT (s)
90
105
120
135
150
165
Depth (m)
Chirp Line 48
~2 km
Just West of Siltcoos Bank
Protruding
Hardgrounds
Hardgrounds
Folded strata
Folding
Syncline
Hardgrounds
Paleovalley

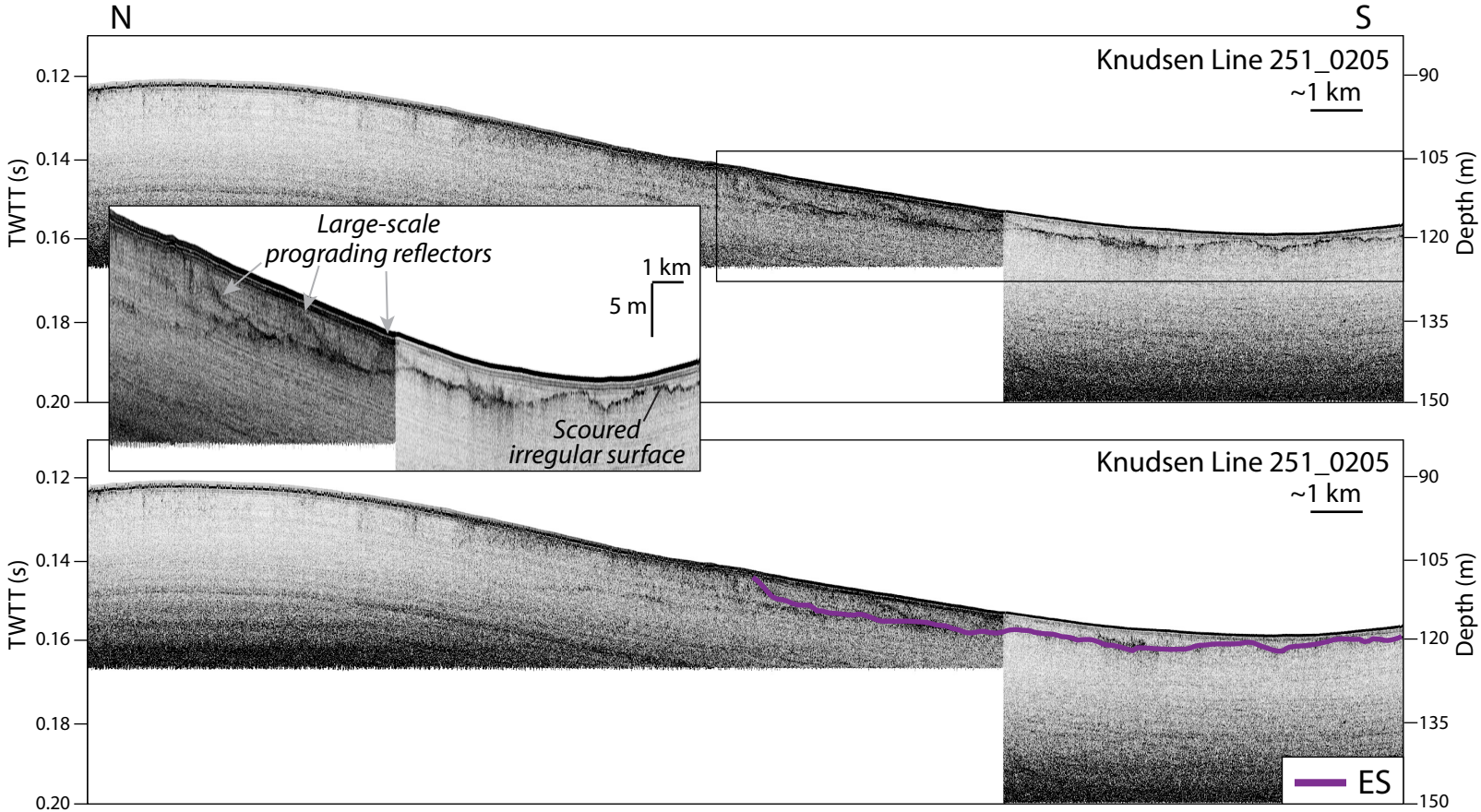
N
S
Knudsen Line 251_0205
~1 km
TWTT (s)
Depth (m)
0.12
0.14
0.16
0.18
0.20
90
105
120
135
150
Large-scale
prograding reflectors
1 km
5 m
Scoured
irregular surface
Knudsen Line 251_0205
~1 km
ES

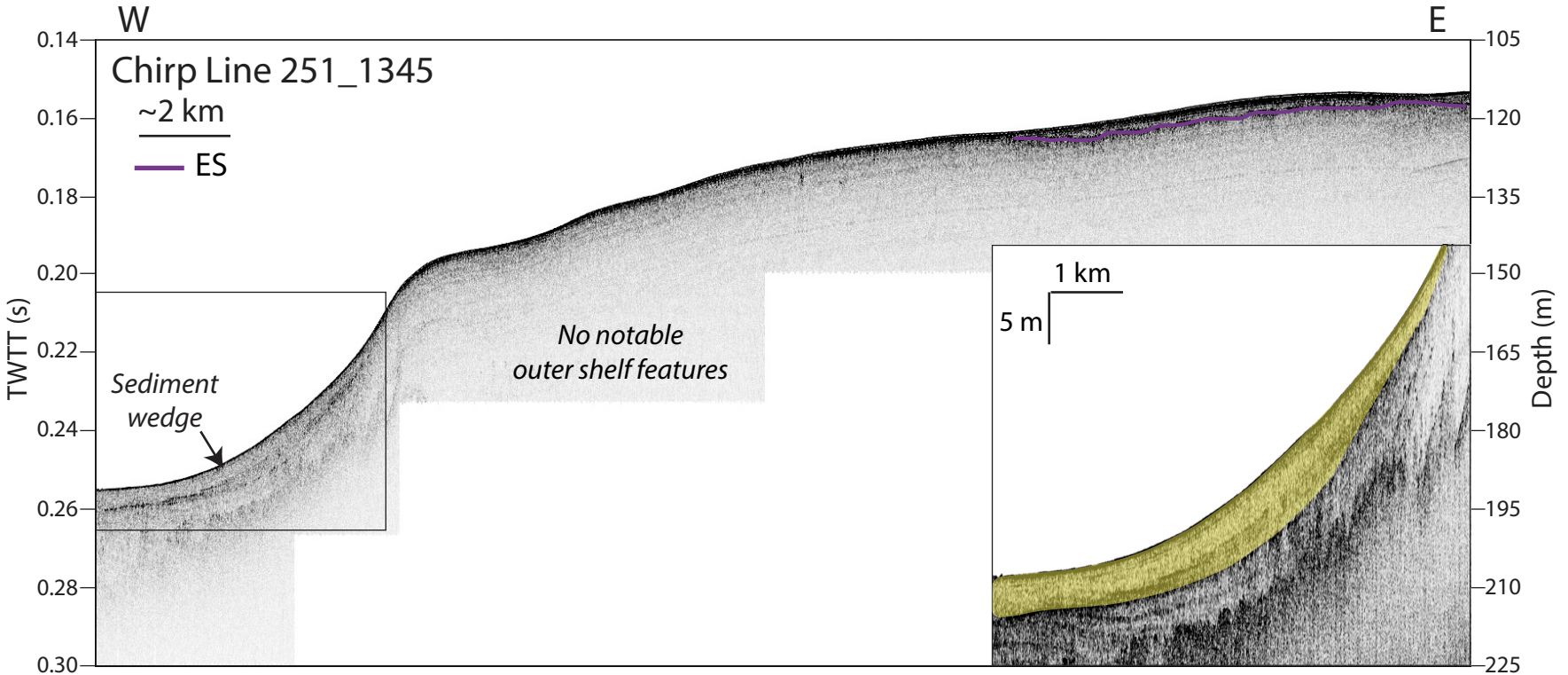
W
E
Chirp Line 251_1345
~2 km
ES
TWTT (s)
0.14
0.16
0.18
0.20
0.22
0.24
0.26
0.28
0.30
Depth (m)
105
120
135
150
165
180
195
210
225
Sediment wedge
No notable outer shelf features
1 km
5 m

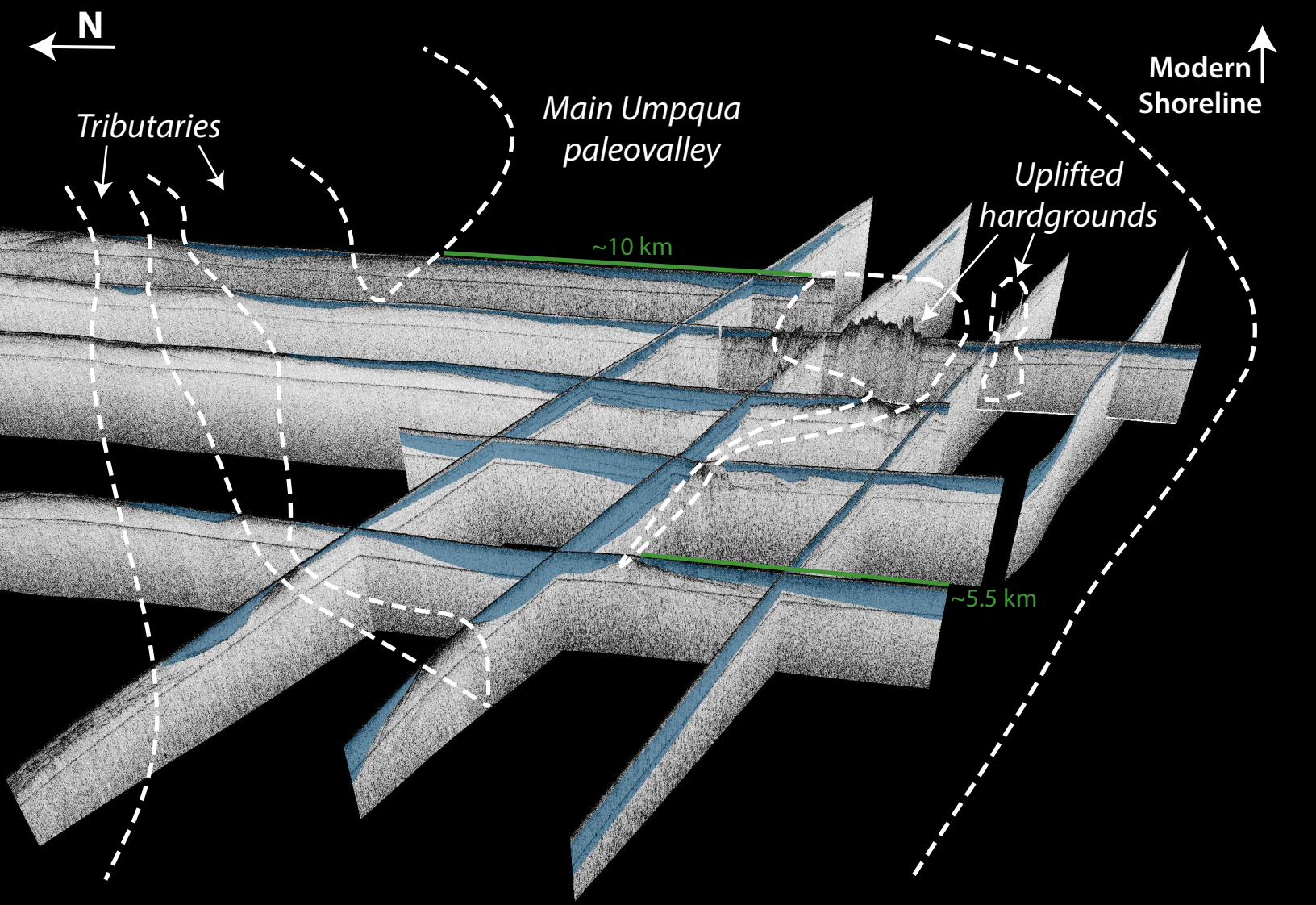
N
Tributaries
Main Umpqua paleovalley
Modern Shoreline
Uplifted hardgrounds
~10 km
~5.5 km

Modern Fluvial Morphology								Continental Shelf Morphology	
River	Highest Elevation (m)	Total River Length (km)	Distance from Headwaters to Mouth (km)	Slope (%)	Drainage Basin Area (km^2)	Average Annual Discharge (km^3/yr)	Sediment Yield ($tons/km^2/yr$)	Slope (%)	Width (km)
Siuslaw	194[b]	177[d]	80[a]	0.11[b]	2,002[h]	2.09[c]	105[e]	0.42[b]	34.8[b]
Umpqua	1828[b]	303[g]*	146[a1],185[a2]	0.05[b]	12,103[g]	8.38[c]	340[f]	0.64[b]	22.8[b]

[a]Google Earth

[b]NOAA-NCEI Coastal Elevation Model - Central Pacific

[c]Kulm et al. (1975)

[d]Armantrout (2000)

[e]USGS Annual Statistics (1968-1975) - Station #14307620, Mapleton, OR

[f]Wheatcroft et al. (2013)

[g] Wallick et al. (2011)

[h] Siuslaw Basin Council (2000)

*includes Umpqua River length of 179.5 km and South Umpqua River length of 179.4 km

[1]Distance from South Umpqua headwaters

[2]Distance from North Umpqua headwaters

Table 1 – Drainage characteristics of the Siuslaw and Umpqua Rivers and associated continental shelf morphology